Forschungszentrum Karlsruhe
in der Helmholtz-Gemeinschaft

Wissenschaftliche Berichte
FZKA 7363

Anisotropy and Buoyancy in Nuclear Turbulent Heat Transfer – Critical Assessment and Needs for Modelling

G. Grötzbach

Institut für Kern- und Energietechnik

Dezember 2007

Forschungszentrum Karlsruhe

in der Helmholtz-Gemeinschaft

Wissenschaftliche Berichte

FZKA 7363

Anisotropy and buoyancy in nuclear turbulent heat transfer – Critical assessment and needs for modelling

Günther Grötzbach

Institut für Kern- und Energietechnik

Forschungszentrum Karlsruhe GmbH, Karlsruhe

2007

Forschungszentrum Karlsruhe GmbH
Postfach 3640, 76021 Karlsruhe

Mitglied der Hermann von Helmholtz-Gemeinschaft
Deutscher Forschungszentren (HGF)

ISSN 0947-8620

urn:nbn:de:0005-073637

5.6.2008

Explanation and corrigendum to FZKA 7363, p. 22 + 23:

a) Explanation of the arguments in the damping functions in the mixing lengths

The formulations in the van Driest and Cebeci damping functions depend on the kind of normalization which is used. The original van Driest formulation requires in the argument of the exponential function in eq. (3-9) y^+/A , where y^+ is calculated from the local value of the wall shear velocity $u_{\tau loc}=\sqrt{\tau_{wloc}/\rho}$.

In eq. (2-8) the integral u_τ is introduced in the normalization of all terms; to avoid misunderstanding this better should have been indicated by $\overline{u_\tau}=\sqrt{\overline{\tau_w}/\rho}$. So, the y^+ occurring in eq. (3-9) is not calculated from the local $u_{\tau loc}=\sqrt{\tau_{wloc}/\rho}$, but from the perimeter averaged $\overline{u_\tau}=\sqrt{\overline{\tau_w}/\rho}$; it should therefore better been indicated by $\overline{y^+}$. As the van Driest function requires the local y^+, this value is determined by extending the formula by introducing the local wall shear stress:

$$y\sqrt{\tau_{wloc}/\rho}\,/(A\,\nu) \;=\; y\sqrt{\overline{\tau_w}/\rho}\,/(A\,\nu)\cdot\sqrt{\tau_{wloc}/\rho}\,\Big/\sqrt{\overline{\tau_w}/\rho}$$

Thus, the $\hat{\tau}_w^{1/2}$ introduced in eq. (3-9, 11, 12, 13) is a dimensionless correction factor built by the ratio of the local wall shear stress to the one averaged over all walls at this axial position:

$$\hat{\tau}_w^{1/2} \;=\; \sqrt{\tau_{wloc}/\rho}\,\Big/\sqrt{\overline{\tau_w}/\rho}$$

Thus, averaging this factor along the perimeter of all wetted walls at this axial flow position will result in one.

As the arguments in the exponential function can be normalized independent from the basic equations (2-1) to (2-3), of course, also the local wall shear stress could be introduced so that the correction factor becomes $\hat{\tau}_w^{1/2} \;\equiv\; 1$.

The same holds also for the argument $y_T{}^+$ in the exponential function which appears in the thermal mixing length according to Cebeci in eq. (3-11, 12, 13).

Thus, the meaning of y^+ and $\hat{\tau}_w^{1/2}$, as they appear in eq. (3-9…), depends on the actually used normalization. This can be summarized as follows:

normalization by	meaning of … in eq. (3-9 ...)	
	y^+	$\hat{\tau}_w^{1/2}$
$\overline{u_\tau}=\sqrt{\overline{\tau_w}/\rho}$, eq. (2-8)	$\overline{y^+}$	$\hat{\tau}_w^{1/2}=\sqrt{\tau_{wloc}/\rho}\,\Big/\sqrt{\overline{\tau_w}/\rho}$
$u_{\tau loc}=\sqrt{\tau_{wloc}/\rho}$	y^+	$\hat{\tau}_w^{1/2} \;\equiv\; 1$

b) Correction to the arguments in the damping function of the thermal mixing length

In eq. (3-11, 12, 13) there is a factor $Pr^{1/2}$ missing in the argument of the exponential function of the thermal mixing length according to Cebeci. The three equations read correctly:

$$l_h = \kappa_h / \kappa \; \ell_{Nik}(y/\hat{y}_T)\left\{1-\exp\left(-y_T{}^{+}\,\hat{\tau}_w^{1/2}\,\mathrm{Pr}^{1/2}/B_w(\mathrm{Pr})\right)\right\} \tag{3-11}$$

$$\mathrm{Pr}_t = \frac{\varepsilon_m}{\varepsilon_h} \approx \frac{l_m}{l_h} = \frac{\kappa\,\ell_{Nik}(y/\hat{y})\left\{1-\exp\left(-y^{+}\,\hat{\tau}_w^{1/2}/A_w(h^{+})\right)\right\}}{\kappa_h\,\ell_{Nik}(y/\hat{y}_T)\left\{1-\exp\left(-y_T{}^{+}\,\hat{\tau}_w^{1/2}\,\mathrm{Pr}^{1/2}/B_w(\mathrm{Pr})\right)\right\}} \tag{3-12}$$

$$\mathrm{Pr}_t = \frac{\varepsilon_m}{\varepsilon_h} \approx \frac{\kappa\left\{1-\exp\left(-y^{+}\,\hat{\tau}_w^{1/2}/A_w(0)\right)\right\}}{\kappa_h\left\{1-\exp\left(-y_T{}^{+}\,\hat{\tau}_w^{1/2}\,\mathrm{Pr}^{1/2}/B_w(\mathrm{Pr})\right)\right\}} \tag{3-13}$$

Anisotropie und Auftrieb im turbulenten Wärmetransport in Reaktoranwendungen – Kritische Bewertung und Modellierungsbedarf

Zusammenfassung

Das weite Anwendungsfeld von CFD-Programmen in der Reaktortechnik, z.B. auf die Analyse der diversen Strömungstypen in einem Accelerated Driven System (ADS), erfordert sehr unterschiedliche Eigenschaften der Turbulenzmodelle für den Impuls- und Wärmetransport. An ausgewählten Transportmechanismen werden physikalische Anforderungen an die Modelle erarbeitet, der Stand der Modelle diskutiert, und untersucht, welche Lösungsmöglichkeiten kommerzielle CFD-Programme dazu bieten. Einen Schwerpunkt der Diskussion bilden die bereits früher erworbenen Kenntnisse zur Anisotropie des turbulenten Austausches für Impuls und Wärme besonders in Wandnähe in Kanalströmungen und welche Notwendigkeiten sich für die numerischen Untersuchungen von Kanalströmungen daraus ergeben.

Den zweiten Schwerpunkt bildet der Wärmetransport in auftriebsbeeinflusster Konvektion. Die Wärmestrommodellierung in den großen kommerziellen CFD-Codes basiert alleine auf der Reynolds-Analogie, d.h. auf der Vorgabe geeigneter turbulenter Prandtl-Zahlen. Für Kanalströmungen gibt es dafür viele Korrelationen, die jedoch kaum in der Praxis benutzt werden. Hier wird eine Korrelation für die lokale turbulente Prandtl-Zahl hergeleitet, die vielseitig für Kanalströmungen verwendbar ist und einen weiten Bereich ADS-typischer Wärmetransportvorgänge abdeckt. Es wird aufgezeigt, dass je nach Reynolds-Zahl und molekularer Prandtl-Zahl des Fluids die ortsabhängige Verteilung der turbulenten Prandtl-Zahl besonders in Wandnähe bedeutsam ist und dort korrekte und mit den eventuell verwendeten thermischen Wandfunktionen konsistente Formulierungen erfordert. An Daten aus Direkten Numerischen Simulationen für horizontale Fluidschichten wird verdeutlicht, dass sich die verfügbaren Turbulenzmodelle, also auch das Konzept der turbulenten Prandtl-Zahl, in Naturkonvektion unzureichend verhalten. An Beispielen wird aufgezeigt, welche diesbezüglichen Modellerweiterungen im Forschungszentrum Karlsruhe in den letzten Jahren entwickelt wurden.

Abschließend werden einige der neueren Ergebnisse zu einem Modellvorschlag für den turbulenten Impuls- und Wärmetransport zusammengefasst. Er basiert auf entsprechend erweiterten algebraischen Modellen und benutzt insgesamt vier bzw. fünf Transportgleichungen für Turbulenzgrößen. Nach aller bisherigen Erfahrung aus der Literatur lässt dieser eine wesentlich verbesserte Wärmetransportmodellierung für anisotrope Zwangs-, Misch- und Naturkonvektion in unterschiedlichen Fluiden erwarten und sollte daher in einem CFD-Programm implementiert und analysiert werden.

Abstract

Computational Fluid Dynamics (CFD) programs have a wide application field in reactor technique, like to diverse flow types which have to be considered in Accelerator Driven nuclear reactor Systems (ADS). This requires turbulence models for the momentum and heat transfer with very different capabilities. The physical demands on the models are elaborated for selected transport mechanisms, the status quo of the modelling is discussed, and it is investigated which capabilities are offered by the market dominating commercial CFD codes. One topic of the discussion is on the already earlier achieved knowledge on the distinct anisotropy of the turbulent momentum and heat transport near walls. It is shown that this is relevant in channel flows with inhomogeneous wall conditions. The related consequences for the turbulence modelling are discussed.

The second topic is the turbulent heat transport in buoyancy influenced flows. The only turbulence model for heat transfer which is available in the large commercial CFD-codes is based on the Reynolds analogy. This means, it is required to prescribe suitable turbulent Prandtl number distributions. There exist many correlations for channel flows, but they are seldom used in practical applications. Here, a correlation is deduced for the local turbulent Prandtl number which accounts for many parameters, like wall distance, molecular Prandtl number of the fluid, wall roughness and local shear stress, thermal wall condition, etc. so that it can be applied to most ADS typical heat transporting channel flows. The spatial dependence is discussed. It is shown that it is essential for reliable temperature calculations to get accurate turbulent Prandtl numbers especially near walls. If thermal wall functions are applied, then the correlation for the turbulent Prandtl number has to be consistent with the wall functions to avoid unphysical discretisation dependences. In using Direct Numerical Simulation (DNS) data for horizontal fluid layers it is shown that the turbulent Prandtl number concept and other available turbulence models have serious deficits in this convection type. Some of the respective model improvements are discussed which were recently developed at Forschungszentrum Karlsruhe.

Finally, a sketch for a turbulent momentum and heat transfer model is given which summarizes the experience from literature and our own results. It is based on extended algebraic stress and heat flux models which use in total four or five transport equations for turbulence quantities. According to all experience one may expect that this model will give considerably improved results for the anisotropic transport in forced, mixed, and buoyant convection in fluids with different molecular Prandtl numbers. Therefore, it should be implemented in a CFD code and should be investigated in more detail.

TABLE OF CONTENTS

LIST OF TABLES

LIST OF FIGURES

1 Introduction

Computational Fluid Dynamics (CFD) is nowadays a standard numerical tool in nuclear reactor engineering. This holds also in studies of Accelerator Driven Systems (ADS) which are under development for transmutation of long living fission products into shorter living ones [Cin04]. It is used to plan complex model experiments [Bau01], to perform detailed investigations and interpretations of the experiments [Kne03], and to transfer the experimental findings from model problems like in [Schb05] and [Sti07] to reactor conditions. In ADS, e.g., a wide spectrum of different flow types is involved: There are simple and complex channel flows, like the flow between the fuel pins in the subassemblies, and flows in large pools with or without internal solid structures. The Reynolds numbers, which characterize the flow velocity, range from nearly no flow or laminar conditions up to highly turbulent flows at large Reynolds numbers. The molecular Prandtl numbers, which characterize the relative importance of the diffusivity of momentum over that for heat of the fluid, extend from small values for liquid metals, as they are used for cooling in the nuclear core, over those for air used in air coolers, and those for water, which is often used as a model fluid, up to large values for organic fluids which are sometimes used for cooling circuits in experiments and as it is planned in one ADS reactor concept [Cin04]. The flows may be purely pressure gradient driven, called forced flows, or more or less influenced by buoyancy forces, called mixed flows, or even fully driven by buoyancy. The occurrence of other transport processes like in recirculating flows, or in flows with secondary currents, which are forming vortices in the plane perpendicular to the main flow direction, complicate the requirements to achieve an adequate numerical description of the turbulent momentum and heat transfer in such flows.

There are huge numbers of different turbulence models for the velocity fields available in literature, see e.g. [Rodi93], [Piq99]. The number of models for the turbulent transfer of heat or other scalars is much less, see e.g. [Lau88], [Han02]. The problem is that all turbulence models have only a restricted range of validity, so that a model which could be used for all types of flows does not exist. So, the users of numerical codes have to select the models which are ’adequate’ for their applications. The selection of the suitable models could be done by the hopefully sufficient experience of the users, or by evaluating the recommendations given e.g. in the code manuals or in the Best Practice Guidelines [Cas00]. Of course, none of these models is sufficient for all types of turbulent transfer tasks, especially if the transport of scalars has to be simulated.

A decade ago we used CFD codes which were developed within the nuclear community, and thus the modelling was directly oriented towards the special requirements of the certain nuclear applications. Now, in Germany, mainly commercial codes are used like ANSYS [ANS07] and Star-CD [Star06] which provide models which should be of general interest to many different engineering fields, but which are not concentrating on the demands of liquid metal cooled reactors and on that of strongly buoyancy influenced flows in different fluids. Only a limited number of momentum transfer models is available in the commercial codes and not a single turbulent heat transfer model, except for the turbulent Prandtl number concept applying the Reynolds analogy between the momentum and thermal field. Within the EC-project ASCHLIM an assessment of the performance of the available CFD codes was performed. It was found, as expected, that the more sophisticated heat transfer modelling in

some of the codes from the nuclear community were superior to the commercial codes, and that for liquid metal heat transfer the Reynolds analogy leads indeed to too large errors [Ari04]. In [Grö06], an overview on the consequences of this change in the code basis is discussed together with the resulting needs for further extensions of the commercial codes for ADS applications. There, also hints on the experimental needs are given to validate not only the numerical results of the chosen physical models, but also to validate the user assumptions which need to be introduced to condense the engineering task to a model problem which is finally simulated. Nevertheless, even sophisticated models need further improvements, e.g. for applications to flows in fuel bundles [Bag07] and for buoyancy driven flows [Grö04].

In this report we will concentrate on two generic features, respectively mechanisms, which are of utmost importance in many turbulent transport processes in an ADS: One is the anisotropy of the turbulent momentum and heat transfer near walls in every channel flow; the other one is the buoyancy influence on some of the closure terms appearing in the turbulence models. The related objectives are (1) to deduce the needs for the models from the available knowledge on the transfer features, (2) to discuss problems of some of the existing models, (3) to select some results of recent relevant model developments, and (4) to gather some of the suitable model contributions to an integral concept for an improved turbulent momentum and heat transfer modelling that should be available for ADS applications. The procedure is as follows: As there is no possibility to calculate reliable heat transfer data without an accurate modelling of the momentum transfer, therefore first the turbulent momentum transfer models are considered in chapter 2. Following the classification of the different types of models in the light of the models which are available in commercial codes, we investigate the need for modelling the anisotropic momentum exchange near walls in forced flows and the influence of buoyancy on the turbulent diffusion in the kinetic energy equation. Then we concentrate in chapter 3 on the turbulent heat transfer modelling, giving a classification of those models and discussing some problems and solutions of the turbulent Prandtl number concept which is the only heat flux modelling in the commercial codes. There, we also give some examples for the different types of more suitable heat transfer models and recent model improvements which could be of interest in this context. The objectives and the proposal for the improved modelling are given in chapter 4. – This report is the written supplement to the public seminar presentation of the author at July 10, 2007 at Institut für Kern- und Energietechnik, Forschungszentrum Karlsruhe. Thus, the intention is not to give a detailed overview complemented by comprehensive references, but to give hints on the most important effects and some related more relevant references only.

2 Modelling of turbulent momentum transfer

2.1 Classification of models

The standard turbulence models which are used in the CFD codes by engineers are based on the time averaged or Reynolds Averaged Navier-Stokes (RANS) equations. By introducing time filtering over time scales which are typical for the turbulent fluctuations of velocities, pressure and temperature, the partial differential equations for mass, momentum, and heat are transferred into those for the corresponding mean data for velocity, pressure, and tem-

perature $\overline{u_i}, \overline{p}, \overline{T}$. In case of flows which are transient at scales which are slower than the turbulent fluctuations, ensemble averaging is used instead of time filtering. For constant material property data these equations can be written in Cartesian coordinates x_i as follows:

$$\frac{\partial \overline{u}_i}{\partial x_i} = 0 \tag{2.1}$$

$$\frac{\partial \overline{u}_i}{\partial t} + \frac{\partial}{\partial x_j}\overline{u_i u_j} = \frac{\partial}{\partial x_j}\left[\nu\left(\frac{\partial \overline{u}_i}{\partial x_j} + \frac{\partial \overline{u}_j}{\partial x_i}\right)\right] - \frac{1}{\rho}\frac{\partial \overline{p}}{\partial x_i} - \beta\, g_i\, \Delta\overline{T} \tag{2.2}$$

$$\frac{\partial \overline{T}}{\partial t} + \frac{\partial}{\partial x_j}\overline{u_j T} = \frac{\partial}{\partial x_j}\left(a\frac{\partial \overline{T}}{\partial x_j}\right) + \overline{\dot{Q}} \tag{2.3}$$

Here ρ is the density, ν the molecular diffusivity for momentum, a the molecular diffusivity for heat, g the acceleration due to gravity, β the volume expansion coefficient, and $\Delta\mathrm{T}$ the difference between the local and a reference temperature. The terms in equations (2.2) and (2.3) are from left to right the rate of change term, the convective term, the diffusive term, and the source terms like the pressure gradient, the buoyancy forces, or the specific internal heating rate $\dot{Q}$.

In the non-linear or convective term of the up to three momentum equations (2.2) the averaged product of the velocities is separated by the Reynolds decomposition of the velocities

$$u_i = \overline{u_i} + u_i' \tag{2-4}$$

so that the well known closure problem appears which is the unknown averaged product of the velocity fluctuations:

$$\partial/\partial x_j\, \overline{u_i u_j} = \partial/\partial x_j\left(\overline{u_i}\,\overline{u_j} + \overline{u_i' u_j'}\right) \tag{2-5}$$

As a result of the Reynolds averaging we get a tensor consisting of 9, or due to symmetry reasons of 6 unknown shear stresses, which contain the complete momentum exchange due to the turbulent fluctuations. So models have to be introduced which mimic the complete turbulent momentum exchange in any type of turbulent flow.

Most of the turbulence models are using the eddy diffusivity concept. It is assumed that the turbulent shear should follow a similar law like the molecular shear. For the molecular shear in common fluids the Newton law is applied which links the shear stress by means of the molecular diffusivity ν to the gradient of the velocity. Accordingly, a gradient approximation is formulated for the turbulent shear stresses in which the newly introduced unknowns, the eddy diffusivities for momentum ε_m^{ijkl}, is a tensor of fourth order; for the notation see [Meyd75].

$$\overline{u_i' u_j'} = -\varepsilon_m^{ijkl}\left(\frac{\partial \overline{u}_k}{\partial x_l} + \frac{\partial \overline{u}_l}{\partial x_k}\right) \tag{2-6}$$

Nonetheless, in most simpler and numerically more efficient models we find the anisotropic eddy diffusivity tensor ε_m^{ijkl} replaced by one isotropic scalar diffusivity, ε_m, which means, each shear stress component is governed by the same still unknown turbulent diffusivity. Whether this simplification may be justified in ADS typical flow simulations is considered later in chapter 2.2.1.

modelling order	Isotropic turbulent transport	Anisotropic turbulent transport	Number of transport equations
1st order	**Gradient models, eddy diffusivity models**		
	l mixing length models	$l^i l^j$ mixing length models	0
	k-l, k-ε, k-ω, SST, etc.		1, 2
	non-linear k-eps etc.		2
?		ASM-models with k-ε	2
2nd order	**Transport eq. for all second order closure moments**		
		eq. for complete shear stress tensor	6 + 1

Tab. 2-1: Classification of turbulent momentum transfer models and availability in common commercial codes (marked fields).

Tab. 2-1 gives a classification of the turbulent shear stress models according to their order of approximation and to their isotropic or anisotropic exchange modelling capabilities. The gradient or eddy diffusivity models are called first order models, because there enter the first order statistical moments of the turbulence field into the modelling, see equation (2-6), whereas second order models use modelled transport equations for the second statistical moments, i.e. for the shear stresses themselves. As further information we give the number of additional transport equations which are solved to approximate the closure terms.

Among the first order models which apply isotropic eddy diffusivities ε_m, there are prominent examples. The simplest model is Prandtl's mixing length approach in which a length scale is introduced which depends on wall distance (for references to the cited models see e.g. [Rodi93]). Thus, the eddy diffusivity is formulated exclusively on local geometry parameters. The modelling becomes problematic when wall-free flows have to be calculated like the mixing in jets or buoyant plumes in large containers. In addition, transport phenomena, like turbulence produced in one area and transported to another area, like behind a grid, or in diffusers, cannot accurately be treated by such a zero-equation model, independent on the quality of the mixing length formulation. For such applications models are preferred which solve one, two or more additional transport equations, e.g. for the kinetic energy k of the turbulent velocity fluctuations, for its dissipation ε, for the vorticity ω, or for a length scale ℓ. Even combinations of such models became attractive like the k-ω based SST model [Men93]. The limitations of these more sophisticated first order models become obvious from this classification: There are flows, in which the positions of zero turbulent shear stress and vanishing velocity gradient do not coincide, as it is assumed by models using equation (2-6). Examples are channel flows with non-symmetric wall conditions, e.g. with walls with different wall roughnesses, or annuli with very small ratios of radii. And there are flows in which the turbulent momentum exchange is strongly anisotropic, so that an isotropic eddy diffusivity ε_m is not applicable.

From an academic point of view, the second order models would be the best modelling of flows with anisotropic momentum transfer and counter-gradient momentum fluxes: These models introduce closure approximations within the transport equations for the turbulent shear stresses. Such equations can be formally deduced by starting from the momentum equations, see e.g. in [Don73], but they contain a large number of closure terms. Some of the closure terms are formulated in terms of k and ε, where k can be determined from the sum of the three auto-correlations; so the resulting number of additional equations is 6 + 1. It was expected in the past that such models should be more universal than the first order transport equation models, but introducing closure assumptions on this level of complexity is a real challenge, so that the expected level of universality seems not yet achieved. In addition, the numerical solution of these equations may also be a challenge due to the existence of fast coupling terms between these equations. The usage of this full second order RANS concept requires a considerably increased numerical effort and special knowledge of the users to solve occasionally occurring convergence problems. An assessment of the second order models is given e.g. in [Han99].

The Algebraic Shear stress Models (ASM) form a class of models between first and second order modelling. They are deduced by starting from the full second order transport equations. Local equilibrium between production and destruction is assumed, which means the redistribution terms convection and diffusion can be cancelled out. The remaining closure terms are formulated in terms of k and ε so that the resulting number of additional equations is 2. As a result algebraic simplifications of the full second order differential equations are achieved. These models should be attractive because they form a numerically efficient basis for calculation of flows with anisotropic momentum exchange and counter-gradient momentum fluxes.

The non-linear k-ε models are simplified ASM versions. According to their modelling basis, they are formulated in terms of gradients of the first moments, but as there are additional terms occurring, they have a limited applicability to flows with counter-gradient momentum fluxes and with anisotropic momentum exchange. Compared to the standard k-ε model they give improved results e.g. for flows with secondary currents. The models can also be trimmed to roughly reproduce the buoyancy introduced anisotropic momentum fluxes, see e.g. [Dav90].

The simplest anisotropic first order model is widely neglected; it is based on Prandtl's mixing length approach. In assuming that the mixing length ℓ is also a direction dependent quantity ℓ^i, one has to find adequate mixing lengths in the required directions. Assumptions for fuel bundles were e.g. introduced by [Meyd75]. Such an approach is highly specialised to the certain geometry for which the required mixing lengths expressions were formulated. And, of course it suffers from all usual problems of first order zero-equation models.

The RANS model types which are contained in most of the commercial CFD codes, e.g. in STAR-CD [Star06], are given in Tab. 2-1 in the marked boxes. So we have a large number of models basing on gradient modelling and assuming isotropic momentum exchange coefficients, each one with different advantages and disadvantages. These form the basis for engineering applications. For applications in which non-isotropic exchange coefficients are required, we have only the tricky and expensive full second order models. The much cheaper

compromise of ASM models is missing, but instead we have the non-linear gradient models for flows with weakly anisotropic momentum exchange.

2.2 Anisotropic turbulent transfer in forced convection in channels

2.2.1 Anisotropic transfer in single-phase convection

It is well known that the turbulent velocity fluctuations in channels are anisotropic. E.g., in a straight pipe apart from the axis, the axial velocity fluctuation takes the largest values, the azimuthal one takes the second largest, and the wall-perpendicular one takes the smallest values [Schl65]. Here we choose the coordinates x_i such that *i*=1 indicates the axial or mean flow direction, *i*=2 the azimuthal or spanwise direction, and *i*=3 the radial or wall-perpendicular direction. The question is, has this anisotropy also consequences for the eddy diffusivities? Are these also anisotropic?

This question can be answered by investigating pipe flows with boundary conditions being inhomogeneous in the azimuthal direction. Nikuradse investigated a pipe flow in which he injected milk at one certain wall position [Nik30]. The sketch for the milk emulsion distribution at different transport lengths downstream of the injection position is given in Fig. 2-1. With increasing axial distance from the injection position the milk is transported from the injection point radially and azimuthally towards the opposing side of the channel. Surprising is that the azimuthal transport along the wall seems to be more effective than the radial transport just across the radius. Thus, there is a clear indication, that a passive scalar is transported near the wall much more efficient azimuthally than radially. This means, the eddy diffusivity for a scalar seems to be highly anisotropic near walls.

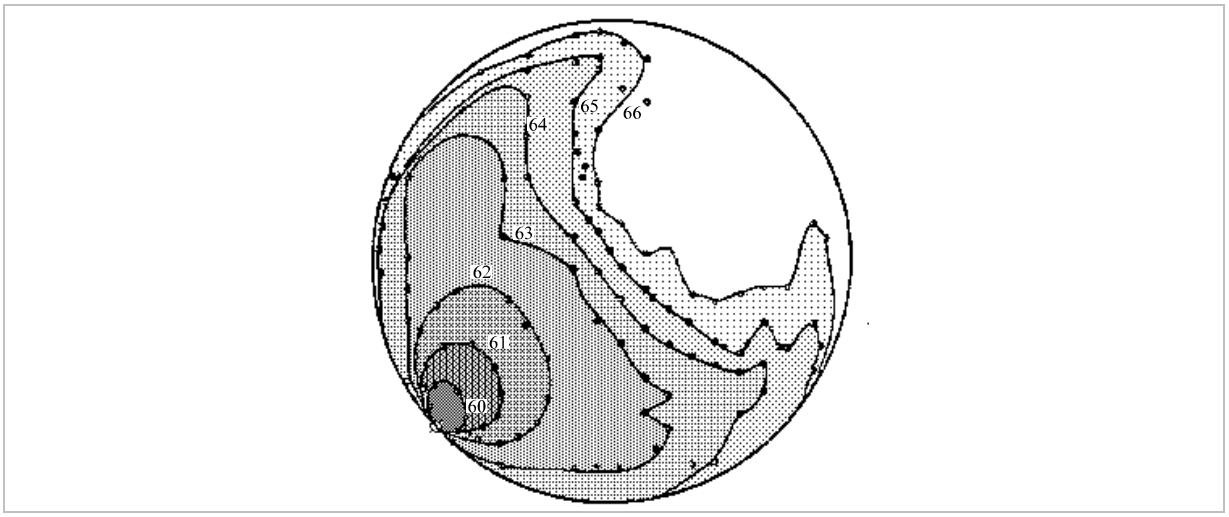

Fig. 2-1 Anisotropic transport of milk in water in pipe flow [Nik30].

The consequence of this anisotropy of the scalar transport can only be observed when there are local sources of the scalars near walls, like here the local injection of milk, or when there are other reasons which cause azimuthal gradients in the mean velocity or scalar fields, like azimuthally varying boundary conditions (roughness parameters or thermal conditions), or non-symmetrical geometrical conditions. Indeed, the detailed thermal and hydraulic investigations for the turbulence in nuclear reactor fuel bundles led in the sixties and seventies to a

major gain in knowledge on the behaviour of the eddy diffusivities in the radial and azimuthal directions. Examples are the publications by [Qua72], [Qua74] considering the radial distribution of the anisotropy ratio of the eddy diffusivity, which is the eddy diffusivity for a scalar in the azimuthal direction divided by the one for the radial direction, $\varepsilon_{h\varphi} / \varepsilon_{hr}$, Fig. 2-2. This ratio is one on the axis of the pipe; it increases slightly towards the wall, but for wall distances below 15 to 20% the increase of the azimuthal diffusivity over the radial one is exponential. The ratio reaches values of about 100 very near the wall! Those authors investigated a wide spectrum of different Reynolds numbers $Re = {}^{b}\overline{u}\, D/\nu$, Prandtl and Schmidt numbers, $Pr = \nu/a$ respectively $Sc = \nu/\gamma$, where ${}^{b}\overline{u}$ = bulk velocity and γ = molecular diffusivity for the transported substance. They conclude that the distribution seems to be independent on these parameters. – Indeed, other publications showed that the anisotropy factor is not fully independent on Re, but that due to changes in the velocity boundary layer thickness there is a weak dependence on Re. This dependence can be removed when the data are not plotted over the relative wall distance $y/(D/2)$, but over the non-dimensional wall distance in units of y$^+$, where D = 2R = pipe diameter, and τ_w = time-mean wall shear stress:

$$y^+ = y/D \cdot \mathrm{Re}_\tau = y\sqrt{\tau_w/\rho}\,/\nu \qquad (2\text{-}7)$$

The shear Reynolds number Re_τ is calculated using the shear velocity $u_\tau = \sqrt{\tau_w/\rho}$. In channel flows it is linked to the common Reynolds number calculated from the bulk velocity by the friction factor C_f:

$$\mathrm{Re}/\,\mathrm{Re}_\tau = {}^{b}\overline{u}/u_\tau = {}^{b}\overline{u}^{+} = 1\Big/\sqrt{C_f/8} \qquad (2.8)$$

From the independence of the anisotropy factor on Pr and Sc one could conclude that this anisotropy is not only a feature of the scalar field, but that it is mainly due to the velocity field. Indeed it was found that this behaviour is also observed for $\varepsilon_{m\varphi} / \varepsilon_{mr}$; see e.g. the overview in [Reh92].

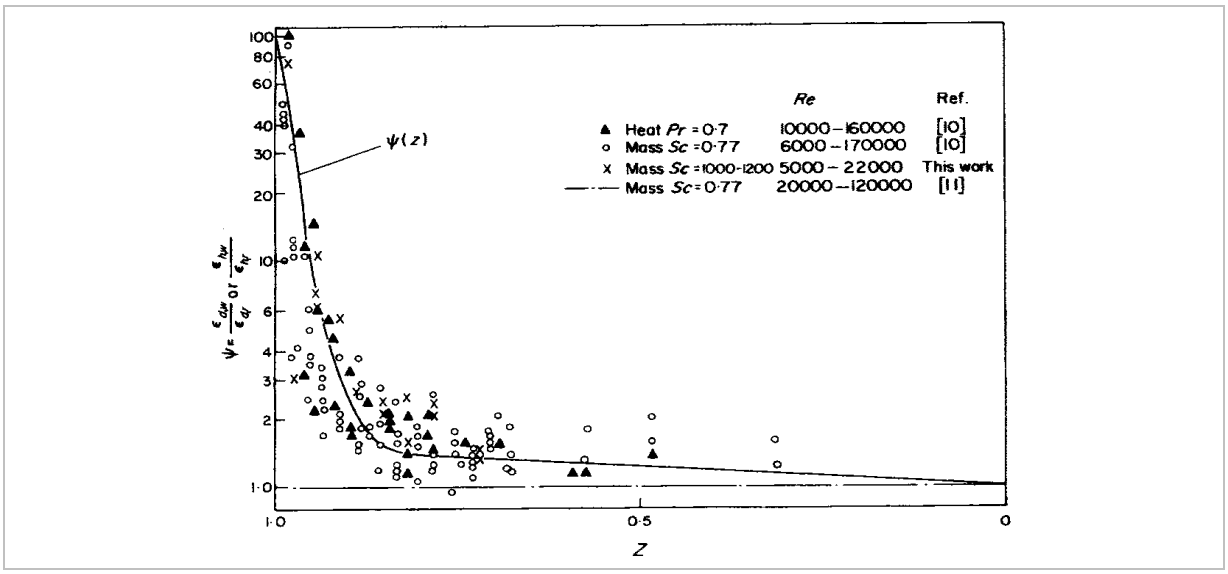

Fig. 2-2 Radial distribution of the anisotropy ratio of the eddy diffusivities for scalars in pipes [Qua74]; Z=r/R.

The mechanisms leading to this anisotropic exchange process can be explained easily: According to equation (2-6) the radial and azimuthal eddy diffusivities are defined in Cartesian coordinates as:

$$\varepsilon_{mr} \hat{=} \varepsilon_m^{1313} = -\overline{u_1' u_3'} \Big/ \left(\partial \bar{u}_1 / \partial x_3\right) \tag{2-9}$$

$$\varepsilon_{m\varphi} \hat{=} \varepsilon_m^{1212} = -\overline{u_1' u_2'} \Big/ \left(\partial \bar{u}_1 / \partial x_2\right) \tag{2-10}$$

So, ε_{mr} designates the radial flux of axial momentum caused by the radial velocity fluctuations, and $\varepsilon_{m\varphi}$ the azimuthal flux of axial momentum caused by the azimuthal velocity fluctuations. As the radial velocity fluctuations are strongly damped near walls due to the presence of the impermeable wall, their momentum is redistributed into the two velocity components parallel to the wall. As a consequence, the velocity fluctuations parallel to the wall have their maximum nearer to the wall than the radial fluctuations, see e.g. [Schl65], [Kaw99]. Thus the azimuthal fluctuations are in the near wall area more effective to transport the axial momentum azimuthally than the radial fluctuations radially.

The necessity of applying anisotropic turbulence models to the velocity and temperature fields in reactor fuel elements was practically observed by several authors already in the sixties and seventies. At that time this was the status quo of the knowledge of those who developed codes for numerical analysis of the velocity and temperature fields in fuel bundles. E.g. Meyder [Meyd75] used an anisotropic mixing length formulation and Ramm & Johannsen [Ramm75], [Ramm75a] used a phenomenological anisotropic eddy diffusivity model to get an adequate reproduction of experimental data for the flow within subassemblies. Later, the knowledge on this necessity was obviously lost in the CFD community in the western hemisphere, whereas there were still publications on this subject in Russia [Bob85] and by experimentalists, see the review by Rehme [Reh92]. Within the last decade groups e.g. in Korea and Japan started with investigations applying commercial codes to the flow in fuel elements. They document, as could have been expected, that the isotropic k - ε model is insufficient to reproduce sufficiently accurate the axial flow in fuel bundles [In03], [Bag03]. They learned again that anisotropic turbulence models are required, and concluded that the non-linear k-ε model might be an acceptable compromise, see e.g. [Bag03]. After further investigations and analysis, Baglietto & Ninokata proposed just recently an improved non-linear model especially for subassembly flows [Bag07].

In densely packed fuel rod bundles with pitch *P* over pin diameter *D* ratios *P/D* below 1.15 there occurs an additional phenomenon which causes efficient mixing between subchannels and which is therefore a challenge for turbulence modelling. In many of the detailed experimental investigations, e.g. by [Hoo84], [Möl92] and [Kra98], there were strong and periodic velocity fluctuations observed in the narrows between the fuel pins. At first, these oscillations in bundle flows were interpreted in different manners, see [Reh92], e.g. as an increased turbulence level. Later [Mey94] could explain the phenomenon by regular vortex patterns in the z-φ-plane which are formed by an instability and which move in the gaps between the pins downstream. They could show that such regular vortex patterns and pulsations are not only occurring in axial bundle flows, but that these are also produced in other compound channels in which wide channels are coupled to very narrow ones, e.g. like in deep river beds coupled to flat flood planes. Now, for laminar flow there is another investigation explaining the phenomenon by an instability [Gos06]. Recalculation of such bundle experiments by stationary

RANS were found a challenge, but reproduction of the strong mixing by this special vortex pattern in a simplified channel by Large Eddy Simulation (LES) was successful [Bie96].

For deciding which simulation method is required for these bundle flows with *P/D* < 1.15, one has to know whether the vortex pattern belongs to the turbulence and should be included in a suitable RANS closure model, or whether it is a separate large scale structure which should be produced as part of the numerical solution by an Unsteady RANS (URANS). As the first case is hardly possible, there the only alternative would really be to use LES. A decision could be tried by comparing the frequency spectra as given e.g. in [Mey94] and comparing them to those in simple channels, e.g. by [Lör77], but the separation of the low frequent vortices from the low frequent turbulence is not very clear. A somewhat clearer result follows from considering directly the time scales: The time scale of the vortex pattern is somewhat larger than the formal integration time to deduce the RANS equations; the latter one could be estimated by means of the Taylor hypothesis from the convection velocity and by means of the two-point correlations of the undisturbed turbulent velocity fluctuations which become zero for distances beyond 1.6 D to 2 D. Thus, as the time scale of the regular patterns is outside the one of turbulence, LES is not really required, but an URANS should be sufficient. And indeed, this rough estimation of the required method is consistent with the finding by [ChaT04] and by [Bag07] that URANS can really reproduce such persistent regular vortex patterns in narrow gaps.

It is hard to define here what belongs to turbulence and what should be considered separately. This is not only a problem for deciding which simulation method should be applied, it is also decisive for the interpretation and comparison of the experimental and numerical results, because the time averaging which is used in both methods might be different. The URANS implies conditional and ensemble averaging; as a consequence here the energy of the regular vortex patterns is not included in the turbulence data. In contrast, in many of the experiments time averaging over longer times has been used, so that the turbulence data may contain the energy of the regular structures.

2.2.2 Anisotropic transfer in two-phase convection

Let us shortly consider whether the strong anisotropic momentum and heat transfer, which was found to be relevant even in simple channels near walls in single-phase flows with inhomogeneous boundary conditions, also exists in two-phase bubbly flows. Such flows occur in some ADS system concepts, which are based on passive cooling, that means, which use mainly buoyancy as a driving force for cooling. To reduce the vertical extension of the reactor vessel and reactor building, the free convection shall be increased by gas bubble injection to increase the active density difference [Ben07].

It could be argued that the interfaces due to the gas bubbles in the flow might reduce the turbulence level and thus may also reduce the anisotropic momentum exchange. In a detailed experimental analysis using X-ray tomography to determine the 2d gas distribution in cross sections of a pipe with D = 70 mm and 5 m length in an air-water system this was investigated by using asymmetric gas injection. In upward directed flow it was found in [Sam96] over a wide range of Reynolds numbers that the resulting gas distribution, Fig. 2-3, indicates transport phenomena which are especially at lower relative volumetric gas content

β very similar to the one found by Nikuradse in his milk experiment, Fig. 2-1. The locally injected gas bubbles are redistributed more efficient in the azimuthal direction than in the radial direction. This effect of the anisotropic exchange is in two-phase flows even augmented compared to the single-phase flow because in upward flow the lift force on the bubbles tends to move the bubbles towards the walls which reduces the radial redistribution. Thus, the large relative local gas content α and the corresponding buoyancy contribution by the bubbles do not reduce the strong anisotropic turbulent mass and scalar transport near the wall in the considered parameter range. Accordingly, the same necessity is found to use anisotropic diffusivities in CFD applications to bubbly flows as in single-phase flows.

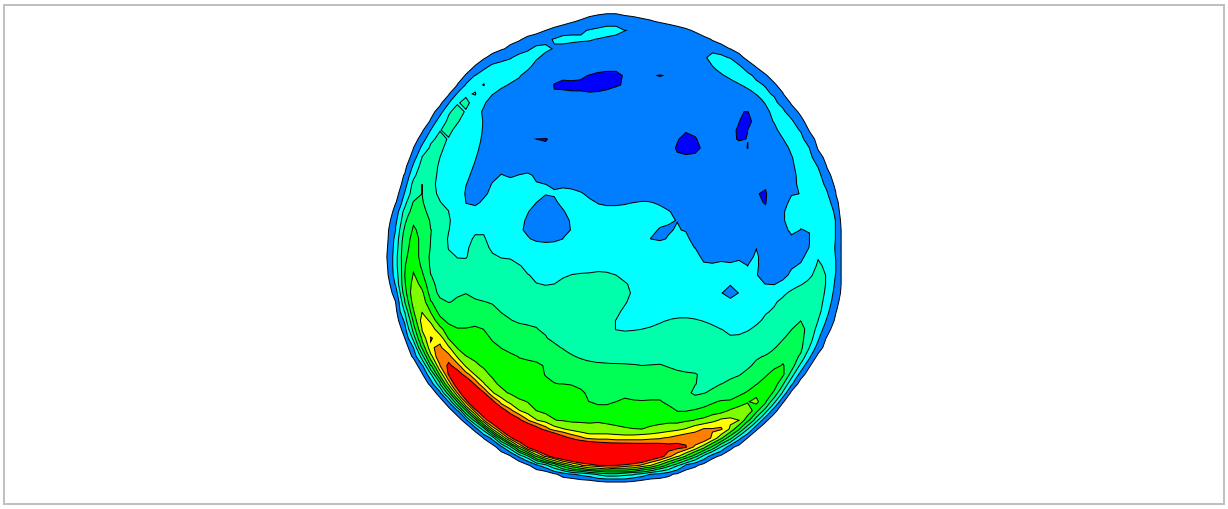

Fig. 2-3 Gas distribution in air-water upward flow at z/ D =63, β=5%, α_{max}≈20% [Sam96].

Thus, the relevance of the anisotropy of the turbulent exchange coefficients near walls for engineering applications of CFD codes is obvious: The anisotropy has to be considered in all applications to single-phase flows and bubbly two-phase flows in which in simple channels the boundary conditions depend on the spanwise coordinate (spanwise = along wall but perpendicular to mean flow direction, here *i*=2). This holds also in channels with a more complex geometry, in which the asymmetry in the geometry leads to wall shear stresses or wall heat fluxes which depend on the spanwise direction. This is especially true for the axial flows in fuel bundles, when low-Reynolds number versions of turbulence models are applied. For calculations which do not resolve the boundary layers of the momentum or scalar fields, modelling of this anisotropy is of reduced importance.

2.3 Buoyancy contributions to closure models

2.3.1 Problem and DNS data base

The influence of buoyancy on turbulence models has been investigated and improved since several decades. There are formal contributions of buoyancy in the basic equations, like the buoyancy force in the momentum equation (2.2) and the production due to the turbulent heat flux in the transport equation for the kinetic energy k (2.11). In addition, there are also implicit contributions to some closure terms in the additional transport equations, which cannot be recognized so directly, but which were concluded to exist because of practical experience with the models. In strongly buoyancy influenced or buoyancy dominated flows there is a

strong coupling not only from the velocity field to the field of the transported scalar, but also back from the scalar field to the velocity field, see equations (2.2) and (2.3). This two-way coupling holds also for the additional closure equations, see e.g. in [Car03]; it makes the investigation and improvement of turbulence models complicated. So, there is still intensive work going on in this field to improve the status quo, see e.g. the review in [Han02]. The current commercial CFD codes account for the formal inclusion of some buoyancy contributions, but the implicit ones to certain closures are not accounted for. This is one of the reasons why the codes have serious deficits in applications to strongly buoyancy influenced flows. Therefore, only the most sophisticated models, the full second order models, are recommended in the Best Practice Guidelines [Cas00] on page 81 for buoyancy influenced flows.

At FZK we were working in several phases since the end of the seventies on improving turbulence models for buoyant flows by using Direct Numerical Simulation (DNS) data from our in-house TURBIT code [Sch75], [Grö87], [Wör94]. Overviews of our earlier work are given in [Sch80], [Grö87], and [Grö99]. DNS means, that we just solve the complete three-dimensional time-dependent basic equations by adequate numerical schemes and on grids which resolve all relevant scales of turbulence: This means, one has to record the largest scales as well as the smallest scales, and one has to record the slowest scales as well as the fastest scales of the turbulence in the flow. Simulations which fulfil these requirements do not depend on any physical models and thus do not depend on any model parameters.

In the following discussion of necessities of current RANS models and the recently developed model improvements for buoyant flows we are using carefully validated DNS data which were generated and analysed in the Institute for Reactor Safety. The data for Rayleigh-Bénard Convection (RBC) in several fluids were published e.g. in [Bun98], [Wör94] and for an Internally Heated fluid Layer (IHL) e.g. in [Grö89], [Wör97]. For each convection type one simulation was added recently in the Institute for Nuclear and Energy Technologies, see e.g. the publications [Oti05] and [Cha07].

The RBC is the convection in a horizontal fluid layer with infinite horizontal extension which is heated from below and cooled from above. The instability of the light hot lower boundary layer develops at larger heating rates plumes convecting upward, and the heavy cold upper boundary layer forms plumes plunging downward. The core of the fluid is roughly isothermal. The vertical section in Fig. 2-4 which is taken from a hologram from Jahn [Jah75] indicates lines of equal density, or for a fluid with a linear dependence between density and temperature, this indicates also the instantaneous temperature field. Here in this example the flow of air is laminar; the pattern indicates to a regular roll pattern which moves the hot fluid upward und the cold one downward. The heat transfer in RBC can be characterized by the Rayleigh number $\mathrm{Ra} = \mathrm{g}\,\beta\,\Delta\mathrm{T_w}\,D^3/(\nu\,a)$ where $\Delta\mathrm{T_w}$ = difference between both wall temperatures, and D = channel height. The numerical results are scaled by using the length scale D, the temperature scale $\Delta\mathrm{T_w}$, and the velocity scale $(\mathrm{g}\,\beta\,\Delta\mathrm{T_w}\,D)^{1/2}$ because this leads to velocity fluctuation amplitudes which are widely independent on the Rayleigh number [Grö82a].

The IHL is also a horizontal fluid layer with infinite horizontal extension, but it is internally heated by homogeneously distributed heat sources within the fluid, and it is cooled by cooling the bottom and top walls. This convection type mimics a nuclear core melt; in this case, the fluid is bounded by its own crusts, so that the lower and upper wall temperatures are

equal and are fixed by the freezing temperature of the melt. The heavy cold lower boundary layer is stably stratified and does not produce any convection. Only the upper heavy cold boundary layer becomes unstable due to Rayleigh-Taylor instability and releases locally some cold plumes which plunge into the hot core. For turbulent flow as given in Fig. 2-4 this plume detachment occurs irregularly. Movies of the transport phenomena in both flow types are given in the DNS databank on the web-page [Wör97a]. The heat transfer in IHL can be characterized by the modified Rayleigh number $\mathrm{Ra} = \mathrm{g}\,\beta\,\dot{Q}\,D^5/(\nu\,a\,\lambda)$ where $\dot{Q}$ = volumetric heat source and λ = thermal conductivity. The scaling of the numerical results is the same as for RBC except for the temperature scale ΔT_{max}: This one cannot be fixed in advance; it is a result of the simulation. Thus, it was estimated in advance by using well known Nusselt number correlations for the IHL as given in [Kul85].

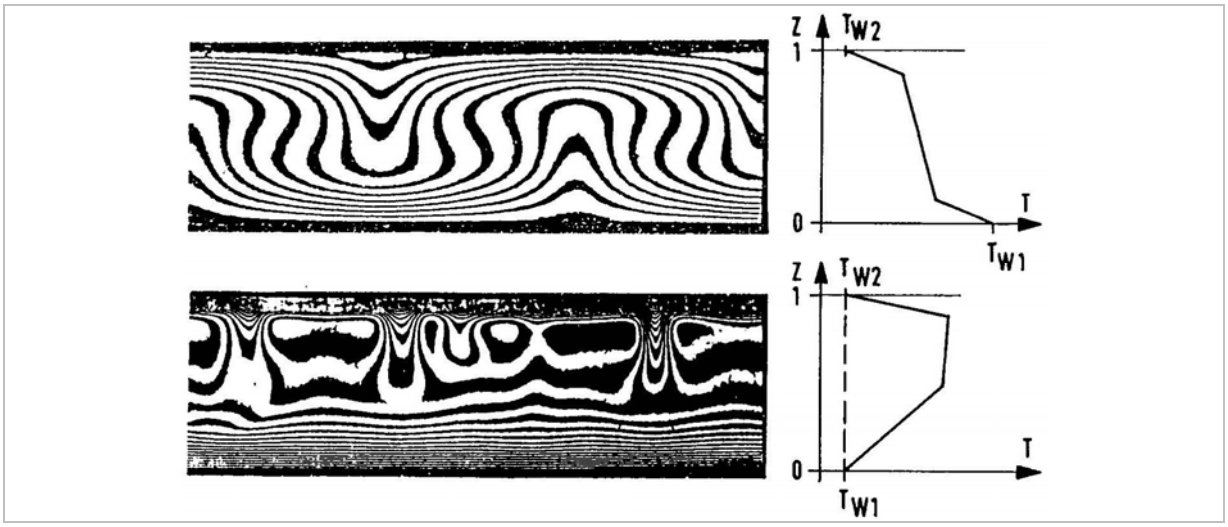

Fig. 2-4 Vertical sections through instantaneous temperature fields in RBC (top) and IHL (bottom) at arbitrary time and position [Jah75] and schematics of time averaged temperature profiles.

For turbulence modelling, the RBC is representative for convection in thermally unstably stratified flows, because turbulence is augmented by buoyancy. At lower Rayleigh numbers temperature inversions may be built up [Grö82a] so that counter-gradient heat fluxes may occur; at large Rayleigh numbers the core of the layer becomes isothermal so that the heat has to be transported with zero temperature gradient. In the IHL we find an unstable layer above the position of the temperature maximum and a stable layer in the complete area below the temperature maximum. In stable stratification the buoyancy is working against the turbulence production leading to damping of turbulence. This causes wide areas in which the heat is transported against the temperature gradient [Grö82], and in which e.g. the kinetic energy k is also transported against its gradient [Wör97]. For a discussion in which types of flows one has to expect such counter-gradient thermal fluxes, see [Sch87]. For RBC there exists an extensive literature with turbulence data to verify a DNS; so we used the simulation of RBC originally to learn how to perform accurate DNS for buoyant convection [Grö83]. The real target of the investigations was to provide data for the IHL by means of reliable DNS, because for this flow there exist up to now from experiments no reliable turbulence data which could be used for model development, except for our own DNS results. An overview on former experimental and numerical IHL investigations is given in [Kul85].

2.3.2 Buoyancy effects on k-diffusion in single-phase flow

Here, we concentrate our discussion on the not directly visible buoyancy contribution to the turbulent diffusion $D_{k,t}$ in the transport equation for the turbulent kinetic energy k as it appears in the standard k-ε model. The k equation for horizontal fluid layers is in non-dimensional form as follows:

$$\left.\begin{aligned}\underbrace{\frac{\partial\,\overline{k}}{\partial t}}_{\text{Rate of change}} + \underbrace{\frac{\partial}{\partial x_j}\left(\overline{u_j}\;\overline{k}\right)}_{\text{Convection}} = \underbrace{-\overline{u_i'u_j'}\frac{\partial\overline{u_i}}{\partial x_j} + \delta_{j3}\overline{u_j'\theta}}_{\mathrm{P_k}} - \underbrace{\frac{1}{\sqrt{Gr}}\overline{\left(\frac{\partial u_i'}{\partial x_j}\right)^2}}_{\varepsilon} \\ + \underbrace{\frac{\partial}{\partial x_j}\left\{\frac{1}{\sqrt{Gr}}\frac{\partial\overline{k}}{\partial x_j}\right\}}_{D_{k,m}} \underbrace{-\frac{\partial}{\partial x_j}\left\{\overline{u_j'k} + \overline{u_j'p'}\right\}}_{D_{k,t}}\end{aligned}\right\} \tag{2.11}$$

Here, $Gr = \mathrm{Ra}/Pr$ and θ is the temperature fluctuation which results from the Reynolds decomposition as used analogously to (2-4) to separate the temperature into a mean value $\overline{T}$ and a fluctuation:

$$T = \overline{T} + \theta \tag{2-12}$$

The production term P_k contains contributions due to the mean shear stresses and due to buoyancy represented by the vertical heat flux; the dissipation term is calculated by the separate transport equation for ε. Thus, the remaining closure terms, which are the triple correlation $\overline{u_j'k}$ and the velocity–pressure fluctuation correlation $\overline{u_j'p'}$ in the turbulent diffusion term $D_{k,t}$, are usually modelled together by assuming gradient diffusion. The unknown eddy diffusivity for the convective energy flux is approximated by a turbulent Prandtl number for k from the eddy diffusivity for momentum, where $\sigma_k \approx 1$ [Lau72]:

$$D_{k,t} = -\frac{\partial}{\partial x_j}\left(\overline{u_j'k} + \overline{u_j'p'}\right) \approx \frac{\partial}{\partial x_j}\left(\left(\frac{\varepsilon_m}{\sigma_k}\frac{\partial\overline{k}}{\partial x_j}\right)\right) \tag{2-13}$$

From practical applications of this model in meteorology it is concluded that the model is insufficient and it is expected that these closure terms are influenced by buoyancy [Moe89]. In addition it is observed in our DNS analyses that in IHL there exist extended areas in which counter-gradient energy fluxes occur which can of course not be reproduced by the gradient model (2-13) and that the model is indeed also insufficient for RBC, see e.g. [Wör97], [Wör98] and [Cha07]. One of the reasons was found in the observation that in most flows the triple correlation gives the dominant contribution, like in IHL, but that in RBC the velocity–pressure fluctuation correlation gives the dominant contribution. Thus, it was decided to try a separate modelling of both terms. By combining two models one should also have a chance to get rid of the problems with the inadequate counter-gradient flux modelling.

The modelling for the velocity-fluctuation triple correlation as given in [Cha07] starts from its transport equation. Therein, indeed formally a buoyancy term containing the triple correlation $\overline{u_j'^2\theta}$ appears as one of the important closure terms. This triple correlation $\overline{u_j'^2\theta}$ also occurs in the convection term as a closure in the transport equation for the turbulent heat flux. Thus an improved modeling of this term is of more general importance. In the investigated horizontal fluid layers the triple correlation is non zero along the vertical direction j = 3. All terms in

the transport equation for this triple correlation are analyzed from DNS data, [Cha05] and [Cha07]. From this analysis a buoyancy-extended version of the Daly and Harlow model [Dal70] is deduced [Cha07a]:

$$\overline{u_3'^2\theta} \approx -C'_{\theta 1}\frac{\overline{k}}{\varepsilon}\left(2\overline{u_3'^2}\frac{\partial\overline{u_3'\theta}}{\partial x_3}+\overline{u_3'\theta}\frac{\partial\overline{u_3'^2}}{\partial x_3}-C_\mu\overline{u_3'^2}\frac{\overline{k}}{\varepsilon}\left(\frac{\partial\overline{u_3'^2}}{\partial x_3}\right)\frac{\partial\overline{T}}{\partial x_3}\;-2\frac{Ra}{\mathrm{Re}^2\,\mathrm{Pr}}\overline{u_3'\theta^2}\right) \tag{2.14}$$

This model is incorporated in the model for the velocity-fluctuation triple correlation.

For the velocity-pressure fluctuation correlation a simple model from Donaldson [Don69] is adopted in [Cha07], in which a coefficient is introduced which depends on the local turbulent Reynolds number. Coupling both models for the closure terms in the turbulent energy diffusion results in the following extended RANS model for the turbulent energy diffusion:

$$\frac{\partial}{\partial x_3}\left\{\overline{u_3'k}+\overline{u_3'p'}\right\}\approx$$

$$-\frac{\partial}{\partial x_3}\left\{\begin{array}{l} C_1\dfrac{k}{\varepsilon}\overline{u_3'^2}\dfrac{\partial k}{\partial x_3} \\ +2\,C_1\dfrac{C_{\theta 1}}{\mathrm{Re}_t^{\beta}}\dfrac{k}{\varepsilon}\dfrac{Ra}{\mathrm{Re}^2\,\mathrm{Pr}}\dfrac{k}{\varepsilon}\left(2\overline{u_3'^2}\dfrac{\partial\overline{u_3'\theta}}{\partial x_3}+\overline{u_3'\theta}\dfrac{\partial\overline{u_3'^2}}{\partial x_3}+\overline{u_3'^3}\dfrac{\partial\overline{T}}{\partial x_3}-2\dfrac{Ra}{\mathrm{Re}^2\,\mathrm{Pr}}\left(\overline{u_3'\theta^2}\right)\right) \\ +\dfrac{C_2}{\mathrm{Re}_t^{\alpha}}\left(\dfrac{k^2}{\varepsilon}\dfrac{\partial\overline{u_3'^2}}{\partial x_3}\right) \end{array}\right\} \tag{2-15}$$

Here three additional closure terms occur: The triple correlations $\overline{u_3'^3}$ and $\overline{u_3'\theta^2}$ can be calculated using models by Launder [Lau89] and by Otić et al. [Oti05], respectively. The third term, $\overline{u_3'^2}$, should be calculated by an additional modelled transport equation e.g. as in Launder et al. [Lau75], but extended by the buoyancy contribution. Thus, this diffusion model extends the k-ε model to a k-ε-$\overline{u_3'^2}$ 3-equation model. It allows for a better representation of the consequences of the large anisotropy on the velocity field which occurs in buoyant flows.

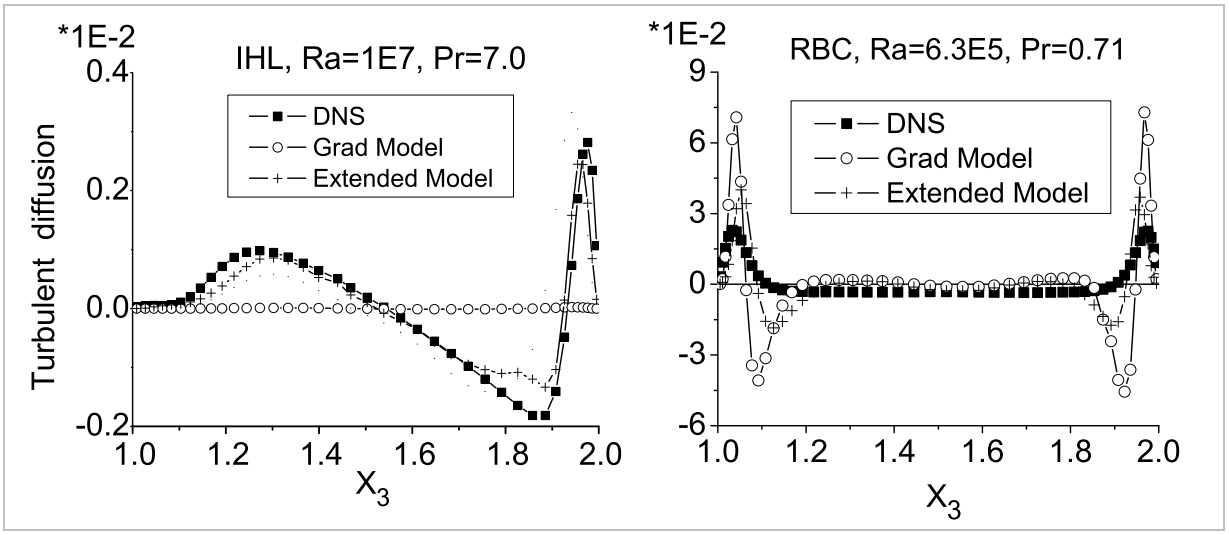

Fig. 2-5 DNS data for the vertical distribution of $D_{k,t}$, for the standard model (2-13), and for the extended model (2-15) [Cha07].

The validation of the extended model against the DNS data in Fig. 2-5 shows that for RBC, the qualitative distribution has only slightly been improved; the diffusion in the core of the flow is still small, but it also still has the wrong sign there. In contrast, for the IHL considerable improvement is achieved, whereas the standard model is completely insufficient. In addition, as the extended turbulent diffusion model is not exclusively based on gradient-diffusion assumptions, it also allows predicting counter-gradient energy fluxes. This follows from the fact that k_{max} is at about x_3≈1.7 [Cha07] and that $D_{k,t}$ is negative above this position, which means energy is transferred downward, against the energy gradient.

This improvement of the turbulent diffusion in the k-equation of the k-ε model should be of general interest for applications to all buoyancy driven flows. To learn whether it is valid also for the velocity fields in buoyancy influenced forced flows, additional investigations should be performed.

2.3.3 Buoyancy in k-equation closures in bubbly flows

In the ADS typical two-phase flows, like in the earlier discussed bubbly flows used to assist the cooling by natural convection, we have buoyancy contributions not only due to temperature differences, but mainly due to the density differences between the liquid and the gas phase. In upward directed flows the bubbles are faster than the liquid and thus a slip between both phases develops. This slip may produce an increase in turbulence energy. On the other hand, the presence of the interfaces may lead to damping of turbulent fluctuations, and thus a reduction of the kinetic energy may occur. Further on turbulence in the liquid phase is also produced by wall shear.

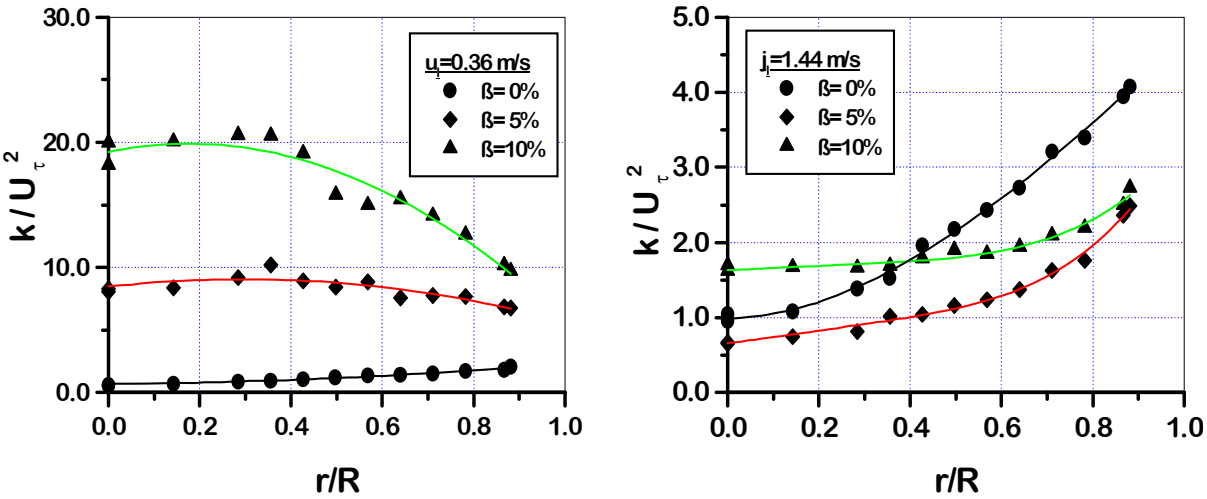

Fig. 2-6 Kinetic energy in air-water upward flow in the liquid phase at z/D=70, β=0%, 5% and 10%, Re≈25.000 and 100.000 [Sam96].

The radial turbulent kinetic energy profiles which are determined by hot film anemometry in the liquid phase by [Sam96] from air-water experiments in a vertical pipe show both phenomena. At large superficial liquid velocities, at j_l=1.44 m/s, the kinetic energy is reduced at small relative volumetric gas contents β near the pipe wall, Fig. 2-6. Obviously, the concentration of gas bubbles near the wall leads in this parameter range at small β values to a damping of the mainly wall shear produced turbulence, compared to the single-phase result,

but with increasing β the kinetic energy increases towards the single-phase values. In the centre of the pipe, where the local gas content is much smaller than β, the tendency is about the same, but the energy may even grow above the value for single-phase flows. At small superficial liquid velocities, at j_l=0.36 m/s, a much higher kinetic energy is found throughout the channel compared to single-phase conditions. This means, the bubble induced turbulence dominates over the wall shear induced turbulence.

The behaviour found in Fig. 2-6 is consistent with the one described by the criterion of Kataoka et al. [Kat93]. The question is, whether standard two-phase turbulence models can predict adequately this complicated production and damping of turbulence due to the buoyancy driven motion of the bubbles. Some answers can be found in analyses by Ilić [Ilic05], [Ilic06] from DNS with the code TURBIT-VoF from Sabisch et al. [Sab01]. From her DNS of bubbly induced turbulence at α=6.5% in a vertical plane channel she found that all models for the production of turbulent kinetic energy by bubbles strongly overestimate the production in this parameter range. The turbulent diffusion is a much more important term than in single-phase flows; all closure models used in engineering codes give much too small turbulent diffusion. The modeling of dissipation in 1-equation models is also incorrect: The dissipation is under predicted at large local gas contents and over predicted at low local gas contents. This means, all closure models used in the kinetic energy equation for bubbly flows need further improvement.

3 Modelling of turbulent heat transfer

3.1 Classification of models

In the time averaged or Reynolds averaged thermal energy equation (2.3) also an averaged product occurs. In the non-linear or convective term the averaged product of velocities and temperature is separated by the Reynolds decomposition (2-4) for the velocities, and analogously by (2-12) for the temperature. So, the well known closure problem appears, the unknown averaged product of the velocity and temperature fluctuations:

$$\partial / \partial x_i \ \overline{u_i T} = \partial / \partial x_i \left(\overline{u_i} \ \overline{T} + \overline{u_i' \theta} \right) \tag{3-1}$$

As a result of the Reynolds averaging we get a vector consisting of 3 unknown heat fluxes, which contain the complete heat exchange due to the turbulent fluctuations. So models have to be introduced which mimic the entire turbulent heat exchange in any type of turbulent flow.

Most of the turbulent heat flux models are using the eddy conductivity concept. It is assumed that the turbulent heat flux should follow a similar law like the molecular heat conduction. For the molecular conduction the Fourier law is applied which links the heat flux by means of the molecular diffusivity a to the gradient of the mean temperature. Accordingly, a gradient approximation is formulated for the turbulent heat fluxes in which the newly introduced unknowns, the eddy conductivities (or eddy diffusivities for heat) ε_h^{il}, should be a tensor.

$$\overline{u_i' \theta} = -\varepsilon_h^{il} \frac{\partial \overline{T}}{\partial x_l} \tag{3-2}$$

Nonetheless, in most models we find the anisotropic eddy conductivity tensor ε_h^{il} replaced by an isotropic scalar one, ε_h, which means, each heat flux component is governed by the same still unknown eddy conductivity. The conditions, for which this simplification may be justified in ADS typical flow simulations, were already considered in chapter 2.2, or more precisely stated: The discussion of Fig. 2-1 and Fig. 2-2 shows, that this simplification may not be applied in all channel flows with inhomogeneous boundary conditions. Thus, more sophisticated anisotropic turbulence models are also required for the scalar fluxes.

modelling order	Isotropic turbulent transport	Anisotropic turbulent transport	Number of transport equations
1st order	**Gradient models, eddy conductivity models**		
	Pr_t Reynolds-analogy		0
	l_h mixing length models	l_h^i mixing length models	0
	k-ε-θ^2, k-ε-θ^2-ε_θ		1, 2
	non-linear AHM		2
?		AHM-models with θ^2 …	1, 2
2nd order	**Transport eq. for all second order closure moments**		
		eq. for complete heat flux vector	3 + 1, 2

Tab. 3-1: Classification of turbulent heat transfer models and availability in common commercial codes (marked field).

In Tab. 3-1 we give a classification of the turbulent heat flux models. This classification widely follows that one which is given in Tab. 2-1 for the turbulent shear stress models. Again the models are sorted according to their order of approximation and to their isotropic or anisotropic exchange modelling capabilities. The gradient or eddy conductivity models are called first order models, because there enter the first order statistical moments of the turbulence field into the modelling, see equation (3-2), whereas second order models use modelled transport equations for the second statistical moments, i.e. for the heat fluxes themselves. As additional information we give the number of additional transport equations which are solved to approximate the thermal closure terms.

The simplest model among the first order models which applies isotropic eddy conductivities ε_h is a modified Prandtl mixing length approach in which a thermal length scale l_h is introduced which depends on wall distance and molecular Prandtl number, see e.g. in [Ceb73]. Thus, the eddy conductivity is formulated exclusively in local geometry parameters. The modelling becomes problematic when wall-free flows have to be calculated like the mixing of a scalar (here heat) in jets or by buoyant plumes in large containers. In addition, transport phenomena, like temperature fluctuations produced in one area and transported to another area, like behind a heated grid, cannot accurately be treated by such a zero-equation model,

independent of the quality of the thermal mixing length formulation. For such applications models are preferred which solve one, two or more additional transport equations, e.g. for the temperature variance $\overline{\theta^2}$ of the turbulent temperature fluctuations. The dimensionless form of the latter is:

$$\underbrace{\frac{\partial \overline{\theta^2}}{\partial t}}_{\text{Rate of change}} + \underbrace{\overline{u_i}\frac{\partial \overline{\theta^2}}{\partial x_i}}_{\text{Convection}} = \underbrace{-2\overline{u_i'\theta}\frac{\partial \overline{T}}{\partial x_i}}_{P_\theta} - \underbrace{\frac{2}{\mathrm{Pr}\sqrt{Gr}}\overline{\frac{\partial \theta}{\partial x_i}\frac{\partial \theta}{\partial x_i}}}_{\varepsilon_\theta} + \underbrace{\frac{\partial}{\partial x_i}\left(\frac{1}{\mathrm{Pr}\sqrt{Gr}}\frac{\partial \overline{\theta^2}}{\partial x_i}\right)}_{D_{\theta,m}} - \underbrace{\frac{\partial \overline{u_i'\theta^2}}{\partial x_i}}_{D_{\theta,t}} \tag{3.3}$$

The closure terms appearing in this equation are the triple correlation in the turbulent diffusion term $D_{\theta,t}$, which was already discussed above with the closures occurring in (2-15), and the dissipation of thermal variance ε_θ. For modelling the dissipation a turbulent time scale ratio R of the thermal to mechanical turbulent time scales could be introduced:

$$R = \frac{\varepsilon}{k} \Big/ \frac{\varepsilon_\theta}{\overline{\theta^2}} \tag{3.4}$$

This allows calculating the required ε_θ from the available dissipation of the momentum field. Specifying the required time scale ratio R near walls and for varying Reynolds, Rayleigh and Prandtl numbers is as problematic as specifying the turbulent Prandtl number which is discussed in chapter 3.2; see e.g. DNS data in [Grö92], [Wör94], [Kas95], [Kaw99], [Schw07]. Thus, to avoid application of this problematic approach when the molecular Prandtl number strongly deviates from unity, an additional transport equation for the dissipation ε_θ is solved, see e.g. in [Nag94]. In chapter 3.3 it will follow that such transport equation models are absolutely necessary for buoyant flows. The limitations of these more sophisticated first order models become obvious from this classification: There are flows like the IHL, in which the positions of zero turbulent heat fluxes and vanishing temperature gradient do not coincide, as it is modelled by equation (3-2), or in which the heat flux is large despite a zero temperature gradient like in the core of the RBC. Further examples are channel flows with non-symmetric wall conditions, e.g. with walls with different wall roughnesses, or from both sides heated annuli with very small ratios of radii. And there are flows in which the turbulent heat exchange is strongly anisotropic, so that an isotropic eddy conductivity ε_h is not applicable, see chapter 2.2.

From an academic point of view, the second order models would be the best modelling of such flows with anisotropic turbulent heat transfer and counter-gradient heat fluxes: These models use transport equations for the turbulent heat fluxes. They also need a number of closure approximations [Rodi93]. The equations can be formally deduced by starting from the thermal energy equation [Don73]. For buoyant flows there appears a production term which contains the temperature variance $\overline{\theta^2}$, for which an additional modelled form of the transport equation (3.3) is required. And as above with the 3 or 4 equation models, for Prandtl numbers different from one, the dissipation ε_θ of the temperature variance is calculated by a separate transport equation, see e.g. [Car97]. The resulting number of additional equations is 3 + 1 or 2 on the thermal side. As some of the closure terms are formulated in terms of k and ε, these 2 equations from the momentum side are also required. It was expected in the past that such second order models should be more universal than the first order transport equation models, but introducing closure assumptions on this level of complexity is a real challenge, so that the expected level of universality seems not yet to be achieved [Car03].

The Algebraic Heat flux Models (AHM) form a class of models between first and second order modelling. They are deduced by starting from the full second order transport equations for the heat fluxes. Local equilibrium between production and destruction is assumed, so that the redistribution terms convection and diffusion can be cancelled out. The remaining closure terms are formulated in terms of k and ε, and for buoyant flows in addition in terms of the temperature variance $\overline{\theta^2}$ and, for Prandtl different from unity, its dissipation ε_θ. So the resulting number of additional equations is 2 + 1 or 2 + 2. As a result algebraic simplifications of the full second order differential equations are achieved. This type of modelling the scalar fluxes was roughly at the same time developed for subgrid scale modelling in Large Eddy Simulation [SchL76], [Som76], and also for the RANS modelling of scalar fluxes [Mer76], whereas systematic developments for RANS followed later, [Lau88]. These models should be attractive because they form a numerically efficient basis for an approximate calculation of flows with anisotropic heat exchange and counter-gradient heat fluxes. Indeed, it is concluded from applications to mixing in stratified fluids that AHM models form a good and efficient compromise between first and second order models [Rodi87].

The non-linear eddy conductivity models are simplified AHM versions. According to their modelling basis, they are formulated in terms of gradients of the first moments, but as there are additional terms occurring, they have a limited applicability to flows with counter-gradient heat fluxes and with anisotropic heat exchange. There are recently intensive development activities on these types of heat flux models, especially to develop also consistent shear stress models to make the combination fully applicable to buoyant flows, see e.g. [Hat06]. Compared to the standard first order 4-equation models they should give somewhat improved results for buoyant wall shear flows with heat transfer.

The simplest anisotropic first order model is based on Prandtl's mixing length approach. In assuming that the thermal mixing length l_h could also be a direction dependent quantity l_h^i, one has to find an adequate thermal mixing length in the required direction. Such models were to the knowledge of the author in the past not explicitly used, but only some phenomenological approaches were going in this direction, like the one in [Ramm75].

The RANS heat flux model type which is contained in commercial CFD codes, e.g. in ANSYS [ANS07] or STAR-CD [Star06], is given in Tab. 3-1 in the marked box. So we have a large number of turbulent heat flux models of very different capabilities in literature, but we have none of them available in our working horses! The modelling which is available uses no explicit model but the Reynolds analogy which assumes that there is similarity in the turbulent transport features of momentum and heat, and that the eddy conductivity is proportional to the eddy diffusivity. The proportionality factor is the turbulent Prandtl number which we will discuss in the next chapter. This means, we have highly sophisticated turbulent momentum transfer models in our commercial codes, up to second order, solving a large number of additional transport equations, but the turbulent transfer of the scalars is calculated by using one factor, which is mostly assumed to be constant in space! As to be expected, it is now standard knowledge that this type of scalar flux modelling is problematic in liquid metal heat transfer applications, and that it fails completely in modelling buoyant flows, where the temperature field gives the source term for any convective transport and needs therefore increased accuracy in modelling.

3.2 Turbulent Prandtl numbers – Status quo in commercial CFD codes

3.2.1 Challenges in modelling turbulent Prandtl numbers

The most widely used method to calculate the turbulent heat fluxes is based on the Reynolds analogy. This assumes similarity in the turbulent transport features of momentum and heat, and thus the eddy conductivity introduced in (3-2) is assumed to be proportional to the eddy diffusivity. The proportionality factor is the inverse of the turbulent Prandtl number Pr_t :

$$\overline{u_i'\theta} = -\varepsilon_h^{il}\frac{\partial \overline{T}}{\partial x_l} \approx -\varepsilon_h\frac{\partial \overline{T}}{\partial x_l} = -\frac{\varepsilon_m}{\mathrm{Pr}_t}\frac{\partial \overline{T}}{\partial x_l} \tag{3-5}$$

$$\mathrm{Pr}_t = \frac{\varepsilon_m}{\varepsilon_h} \tag{3-6}$$

There is very much known about the behaviour of Pr_t in very special and mostly simple flows and for certain fluids. Even the influence of stratification was recently reconsidered [Ven03]. And there are very good reviews on the subject, but these are mostly older literature [ReyA75], [Kay94]. The last major one known to the author is the one by Kays [Kay94]. It is often referred to it, but obviously there are too many correlations discussed, so that most users just apply further on the default value given in the codes, which is a constant value of $\mathrm{Pr}_t = 0.9$. In addition, in many papers some kind of postulated improvements are discussed, but most of them give no progress for other applications. Nevertheless, the use of the concept is essential in our current CFD codes. Therefore, we will give here a short discussion of the problems with the turbulent Prandtl number concept, show how easy it can be to get an approximation for turbulent channel flows of different fluids, and what the limitations of such simple approximations are, and we discuss the relevance of using good wall-distance dependent Pr_t approximations. In the subsequent chapter 3.3 we will see how the problem could be circumvented by existing and recently improved real turbulent heat flux models.

Typical problems with the turbulent Prandtl number concept which are obvious from theory and which appear in practical applications of this concept are manifold; examples are as follows:

- The similarity in the transport features implies also similarity in the statistical features of the velocity and temperature fields. This assumption is often violated, e.g. in channels with one adiabatic wall. There, neither the first statistical moments of u_1 and T are similar, nor their second moments.

- The spatial dependence of both eddy diffusivities may be different. E.g., even for Prandtl numbers around unity, the boundary layer thicknesses of u_1 and T are not the same.

- Smaller modelling deficiencies may become irrelevant with increasing Reynolds number. So, what is the dependence of Pr_t on the Reynolds number?

- With molecular Prandtl numbers Pr differing from one, the thickness of the thermal boundary layer becomes very much different from that one of the velocity field. Thus, similarity does really not exist. Accordingly, most of the investigations of the dependence

of Pr_t on the molecular Pr are mainly motivated by the applications to liquid metal cooled nuclear reactors.

In the discussion below we will show, that these four problems can in principle be overcome for some not too complicated channel flow applications. The following problems are more challenging:

- The sources for producing additional local velocity or temperature fluctuations may be at different places, e.g. by strong local heating, so that there is no proportionality between the two fields. How to model these differences in the transport features, e.g. in diffusers or in recirculating flows?

- In many applications the development status of the velocity field is very much different from the one of the temperature field, because heating starts often not at the inlet into a test section, but somewhat downstream. How to treat the non-similarity due to these differences in the development features?

- It was observed that Pr_t also has some dependence on buoyancy influences, especially if stable stratification is engaged. How to generalize the formulation for this influence of buoyancy between forced, mixed, and pure buoyant convection with any stratification?

- We already discussed the necessity to model anisotropic turbulent momentum and heat transfer in channel flows near walls with inhomogeneous boundary conditions. How to apply there the Pr_t concept?

- And there are applications where counter-gradient heat fluxes occur in other, wider or smaller regions than the counter-gradient shear stresses occur in the momentum field. Should one really apply locally negative values of Pr_t and how to model this?

In the following we will deduce a simple, but a useful and accurate formula to calculate Pr_t for channel flows. After the many publications on this subject one cannot be sure whether this is an original contribution. We will see later, that after two simplifications of the resulting more general model we get a simpler one, which already exists in literature.

3.2.2 A turbulent Prandtl number formula for channel flows

Starting from the definition equation (3-6) we introduce for both diffusivities the simplest turbulence models which we have for channel flows, the Prandtl mixing length concept. The eddy diffusivity for momentum follows e.g. from [Schl65], the eddy diffusivity for heat from [Ceb73]:

$$\mathrm{Pr}_t = \frac{\varepsilon_m}{\varepsilon_h} \approx \frac{l_m^2 \left|\frac{\partial u}{\partial y}\right|}{l_m\, l_h \left|\frac{\partial u}{\partial y}\right|} = \frac{l_m}{l_h} \tag{3-7}$$

For simplicity we use here a one-dimensional nomenclature with u = mean velocity and y = wall-perpendicular direction.

As an acceptable mixing length distribution for momentum l_m we select that one with which the universal velocity profiles can be reproduced best, i.e. the Nikuradse parabola [Nik32], where $\hat{y}$ denotes the 'profile length' which is the distance of the velocity maximum from the corresponding wall:

$$\ell_{Nik}(y/\hat{y}) = \hat{y}\left\{0{,}14 - 0{,}08\left(1-\frac{y}{\hat{y}}\right)^2 - 0{,}06\left(1-\frac{y}{\hat{y}}\right)^4\right\} \tag{3-8}$$

It is known that near walls all mixing length models give too large values, i.e. for y^+ below about 26 to 30. Therefore these models are usually combined with the van Driest damping function [Dri56].

$$l_m = \ell_{Nik}(y/\hat{y})\ \left\{1-\exp\left(-y^+\,\hat{\tau}_w^{1/2}/A_w\left(h^+\right)\right)\right\} \tag{3.9}$$

The van Driest damping coefficient $A_w(h^+)$ depends on the wall roughness parameter h^+ [Grö77]; for smooth walls we get $A_w(h^+=0) = 26$. The arguments in the exponential function in (3.9) are made dimensionless as discussed with equations (2-7) and (2.8); this means we use the length scale D and the shear velocity $u_\tau = \sqrt{\tau_w/\rho}$ to get the dimensionless wall shear stress $\hat{\tau}_w$. In case of inhomogeneous wall conditions one has to use the local value of τ_w at the specific axial and spanwise position. This combination works well in RANS in bundle flows [Meyd75] as well as in a subgrid scale model in plane channels and annuli with inhomogeneous wall conditions [Grö77].

As an acceptable mixing length distribution for heat l_h we select that one with which the universal temperature profiles can be reproduced best, i.e. again the Nikuradse parabola (3-8), but it contains hidden in its coefficients the Karman constant for the momentum field, $\kappa = 0.4$. Therefore, this expression has to be corrected to introduce the value of the Karman constant for the thermal field, $\kappa_h =$ 0.43 to 0.47. Here, this value is a critical one; it has to be consistent with the value of κ_h which is used in the logarithmic law for the dimensionless temperature profile T^+ [Kad81] when a high Peclet number formulation of the turbulent heat flux model is applied which means, when the conductive sublayer is not resolved but a thermal wall function is used instead. The dependence of l_h on the molecular Prandtl number of the fluid is introduced by the Cebeci damping function [Ceb73] employing a coefficient $B_w(Pr)$ according to Na and Habib [NaHa73],

$$B_w(\mathrm{Pr}) = \sum_{i=1}^{5} C_i\,\left(\log_{10}\mathrm{Pr}\right)^{i-1}, \tag{3.10}$$

where C_1=34.96, C_2=28.79, C_3=33.95, C_4=6.33, C_5= -1.186. Thus, l_h is calculated by

$$l_h = \kappa_h \Big/ \kappa\ \ \ell_{Nik}(y/\hat{y}_T)\left\{1-\exp\left(-y_T{}^+\,\hat{\tau}_w^{1/2}/B_w(\mathrm{Pr})\right)\right\} \tag{3.11}$$

where $\hat{y}_T$ denotes the thermal 'profile length' which is the distance of the temperature maximum or minimum from the corresponding cooled or heated wall. Thus we get for the turbulent Prandtl number the following expression:

$$\mathrm{Pr}_t = \frac{\varepsilon_m}{\varepsilon_h} \approx \frac{l_m}{l_h} = \frac{\kappa\,\ell_{Nik}(y/\hat{y})\left\{1-\exp\left(-y^+\,\hat{\tau}_w^{1/2}/A_w\left(h^+\right)\right)\right\}}{\kappa_h\,\ell_{Nik}(y/\hat{y}_T)\left\{1-\exp\left(-y_T{}^+\,\hat{\tau}_w^{1/2}/B_w(\mathrm{Pr})\right)\right\}} \tag{3-12}$$

The Nikuradse parabola $\ell_{Nik}(y/\hat{y})$ for l_m contains the relative distance $y/\hat{y}$ from the wall. The Nikuradse parabola $\ell_{Nik}(y/\hat{y}_T)$ for l_h contains the relative distance $y/\hat{y}_T$ from the wall.

Thus, the model includes the influence of the type of thermal boundary conditions, because in a plane channel with an adiabatic wall the thermal profile length is the complete channel width, whereas the momentum profile length is about half the channel width.

The validity range of this simple RANS model for the turbulent Prandtl number follows from the validity range of the introduced assumptions. It holds for channel flows like pipes, plane channels, annuli or fuel bundles (when the local wall shear stress is used). It holds for smooth and rough walls, and for all types of thermal wall conditions like symmetric and asymmetric heating and cooling. It can be applied at all wall distances, for all Reynolds numbers with turbulent flows, and for all Prandtl numbers $Pr \geq 0.02$. On the limiting side we should remember that the introduced models hold only for stationary and fully developed flow and that they are not applicable to detached and recirculating flows.

For completeness it shall be mentioned, that the Pr_t formula given in eq. (3-12) may not be applied directly to subgrid scale (SGS) models used in LES, because there the introduced integral approximations do not apply. Values for Pr_{tSGS} are for $Pr \approx 0.7$ in the range around 0.4; they can be deduced from the energy spectra or from the theory to calculate the coefficients C_2 of the momentum model and C_{T2} of the heat flux model of the subgrid scale model as it is used in the TURBIT code, see e.g. in [Grö77] and [Grö99]: $\mathrm{Pr}_{tSGS} = C_2 / C_{T2}$, where radial profiles of the coefficient C_{T2} are given for the turbulent core of channel flows for different Prandtl numbers in [Grö81] or [Grö87]. For decreasing Prandtl and Peclet numbers the theory reliably describes the gradual and local transition to fully resolved temperature fields, i.e. to DNS of the thermal field, because the calculated Pr_{tSGS} tends to infinity.

3.2.3 Validation of the formula

The validation of a simplified version of the model (3-12) is given by [Ceb73]. His model, which was deduced by other assumptions, follows from the more general model (3-12) by assuming smooth walls and by assuming symmetric thermal boundary conditions so that the two profile lengths become equal and the two Nikuradse lengths cancel out. Cebeci gives:

$$\mathrm{Pr}_t = \frac{\varepsilon_m}{\varepsilon_h} \approx \frac{\kappa \left\{1 - \exp\left(-y^+ \hat{\tau}_w^{1/2} / A_w(0)\right)\right\}}{\kappa_h \left\{1 - \exp\left(-y_T{}^+ \hat{\tau}_w^{1/2} / B_w(\mathrm{Pr})\right)\right\}} \tag{3.13}$$

Unfortunately, many of the earlier experimental results on turbulent temperature field statistics are seriously wrong as has been shown by Lawn in a consistency check by means of the heat flux correlation coefficient [Law77]. He found for forced channel flows correlation coefficients between 0.1 and 2, whereas the theoretically expected values [Law77] and those from DNS/LES [Grö81] are between 0.4 and 0.5. Thus, data on Pr_t are often not very accurate because evaluation of the data requires according to (3-6), (3-5) and (2-9) the measurement of the shear stress and of the heat flux, as well as the calculation of the gradients of the measured velocity and temperature profiles. So, comparisons of direct results from Pr_t formula to experimental data for this quantity have in general to be taken with care. Much more important is therefore to ensure that the temperature profiles are reproduced well. Cebeci [Ceb73] showed that integration of the thermal energy equation with his simplified wall distance dependent approximation for Pr_t produces temperature profiles which follow accurately the universal temperature profiles, that consequently adequate Nusselt numbers are predicted, and that also some experimental data for Pr_t are well reproduced, Fig. 3-1.

A further validation for the concept of applying the two different profile lengths for the velocity and temperature field in formula (3-12) can be deduced from the performance of our TURBIT code. There these mixing lengths and these profile lengths formulations are also used in the inhomogeneous subgrid scale models which become important in LES using coarse grids for forced flows. The mixing lengths formulations were applied to flows at different Reynolds numbers in plane channels with smooth walls and on those with a roughened wall on one side only, as well as to annuli with very different ratios of radii, both with symmetric heating or cooling or with asymmetric thermal boundary conditions involving heating on one side and the other wall being adiabatic, heated or cooled. In all these applications this profile length concept well reproduced experimental data for velocity and temperature profiles [Grö77], [Grö81].

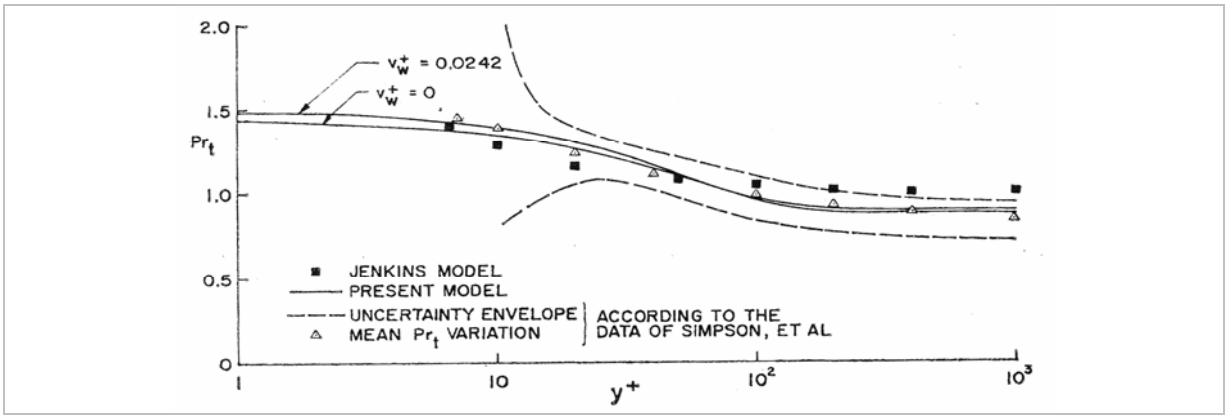

Fig. 3-1: Validation of simplified (3-12) for Pr = 0.71 by Cebeci [Ceb73].

Thus, we have obviously good possibilities to get simple and accurate expressions for the turbulent Prandtl number for certain applications; nonetheless, none of these are available in our commercial codes.

3.2.4 More sophisticated formula

To solve the next two of the remaining problems, which were listed in chapter 3.2.1, that of modelling transport features and that of treating developing flows, needs a much more sophisticated approach. Starting from the modelled transport equations for the second moments of the turbulence and thermal field, Jischa and Rieke [Jis79], [Jis82] deduced a Pr_t model which does not depend on wall distances but on local turbulence parameters. Therefore, it should also be applicable to recirculating flows, jets, mixing layers, etc. This model was applied by one benchmark participant from CRS4 within the ASCHLIM project [Ari04] to the recalculation of the TEFLU sodium experiment [Kne93], [Kne98] which is the mixing of a hot jet in a highly turbulent surrounding co-flow. It was found, that the Jischa correlation gives a better approximation, but not a sufficient one, whereas the other benchmark participants failed to reproduce sufficiently accurate data by using constant turbulent Prandtl numbers. Results of a full second order heat flux model to this benchmark are given in chapter 3.3.

The remaining problems discussed in the list in chapter 3.2.1 can only be solved practically by avoiding the turbulent Prandtl number concept, e.g. by applying suitable 4-equation models, AHM, or even second order turbulent heat flux models.

3.2.5 Local relevance of space dependent formula

Next, we will investigate the relevance of using adequate spatial distributions of Pr_t . In general, the turbulent Prandtl number is used in CFD to model the turbulent heat flux and thus to calculate the spatial distribution of temperature in the fluid. Therefore, from a theoretical point of view the spatial distribution of Pr_t has to be accurate so that e.g. the non-dimensional universal temperature profiles as summarized e.g. by Kader [Kad81] for channel flows are theoretically well reproduced when a given formula, here (3-12), is used together with (3-5) in the integration of the temperature equation (2.3). When the temperature data are well reproduced, then the calculated Nusselt numbers are automatically accurate, see e.g. the validation procedure chosen by Cebeci [Ceb73]; the opposite conclusion does not hold. A second condition occurs when wall functions are used to model the time-mean wall heat fluxes q_w in high Peclet number formulations: The wall functions use certain formulations for the universal temperature profiles, i.e. for the dimensionless time-mean wall temperature difference T^+. The definition is $T^+ = (T-T_w)/T^*$ with the time mean of the wall temperature T_w and of the friction temperature $T^* = q_w / (\rho\, c_p\, u_\tau)$, where c_p = specific heat at constant pressure. On the other hand we just mentioned that the radial Pr_t distribution also results in a certain temperature profile. Thus, in case of applying wall functions in the wall conditions, the formula for the turbulent Prandtl number has to be completely consistent with the corresponding wall law. This means, the Pr_t formula must be able to exactly reproduce the applied wall function. Otherwise, a grid dependence of the CFD results will occur because the calculated temperature profiles will depend in an unphysical manner on the spatial resolution of the grid in the direction perpendicular to the wall.

In Fig. 3-1 we saw that the spatial distribution of Pr_t over the wall distance y^+ gives roughly constant values in the turbulent core of the flow, i.e. at $y^+ > 30$, but near the wall there are more or less strong changes. The recent DNS data in [Schw07] confirm, this distribution and the given scattering band is typical for fluids with $Pr \geq 0.7$. So we will have to investigate whether it is also practically really necessary to deduce formulae for the turbulent Prandtl number which reproduce the changes in their spatial distribution only in a very narrow zone near the wall, that is in the viscous or conductive sublayer and in the thermal buffer layer, whereas in most of the remaining channel indeed a constant value could be applied. For this purpose we consider the temperature profiles or concentration profiles in channel flows with different fluids characterized by the values of the molecular Pr or Sc.

Fluids with $Pr \geq 1$ occur in ADS or respective model systems, e.g. in cooling circuits where water or even organic fluids are applied like in one of the XADS concepts [Cin04] or in the MEGAPIE experiment [Bau01]. Accurate experimental results on temperature data in high Prandtl number fluids are rare because of the extremely thin thermal boundary layer and the small scales in the temperature field. DNS for such fluids need also a tremendous computing power. Recently accurate DNS data became available for concentration profiles with Sc up to 50 in [Schw06] and [Schw07], Fig. 3-2. The logarithmic region of the profile for the dimensionless concentration C^+ (analogue to T^+ in heat transfer) starts as is well known [Kad81] for Sc=1 at about y^+=30, but with increasing Sc it extends nearer to the wall. For the highest Sc number included in the figure, for Sc=25, the increase in the concentration profile is in the near wall area very steep so that already at values of y^+=5 around 90 to 95% of the maximum value C^+_{max} are achieved. This means, we have an extremely steep gradient of C^+ near

the wall. In considering equation (3-5) it follows from the multiplication of $1/\mathrm{Pr}_t$ by the temperature gradient that the only region in which Pr_t has to be highly accurate is exactly this thin near wall range! The values of Pr_t predicted for the inner region are at these Pr or Sc irrelevant because there the gradient is negligible. Unfortunately we also learned from Fig. 3-1 that the scattering band of the experimental data is largest in this near wall range. – In case of a high Peclet number formulation of the temperature equation, that is, when the conductive sublayer is not resolved but thermal wall functions are used instead, then the value of the turbulent Prandtl number is anyhow more or less irrelevant because this strong gradient is not resolved and predicted, instead the temperature difference between wall and the core of the flow is e.g. at Pr=25 up to 90 to 95% determined by the thermal wall function. Thus, it is not very meaningful to expect accurate local heat transfer data at walls from such a high Peclet number modeling.

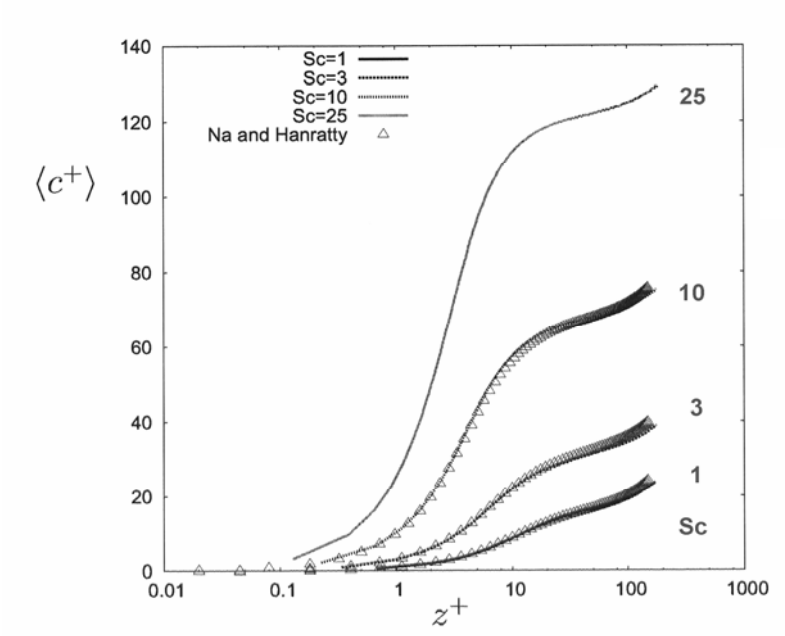

Fig. 3-2 Concentration profiles over wall distance (z^+=y^+) for $\mathrm{Re}_\tau = 180$ from [Schw06].

Fluids with $Pr \approx 1$ are the most common ones in cooling circuits, like hot water or air. Thus most experimental data on temperature profiles are for this Prandtl number. A reformulation of data in universal variables T^+=f(y^+) is given in the standard work [Kad81]. The logarithmic region of the profile starts for Pr=0.7 at about y^+=30, Fig. 3-3. The increase in the profile is in the near wall area also steep so that at values of y^+=5 around 50 to 60% of T^+_{max} are achieved, depending on Re. This means, we have again a steep gradient of T^+ near the wall. As a consequence the region in which Pr_t has to be highly accurate is this thin near wall range. The values of Pr_t predicted for the inner region are at this Pr or Sc not completely irrelevant; there the gradient is not negligible, because in that region the temperature is still increasing by about 40% of T^+_{max}. On the other hand we learned from Fig. 3-1 that Pr_t is roughly constant in that inner region. – In case of a high Peclet number formulation of the temperature equation, that is, when thermal wall functions are used, then the value of the turbulent Prandtl number is anyhow irrelevant in the near wall range, because the temperature difference between wall and the core of the flow is to 50 to 60% determined by the wall function, but Pr_t is then still of some relevance in the core of the flow; nevertheless, there a

constant value might be sufficient. Thus, at this Prandtl number the analysis of the local heat transfer to or from walls from such a high Peclet number modeling is mainly governed by the wall functions and only to a minor part by the Pr_t formula.

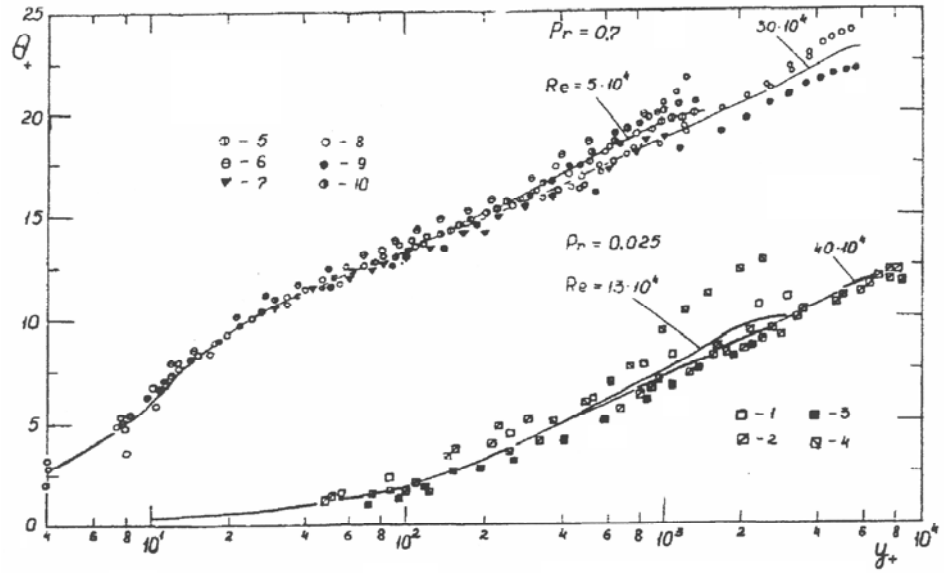

Fig. 3-3 Universal temperature profile ($\theta_+ = T^+$) for Pr=0.7 and 0.025 [Kad81].

Fluids with $Pr << 1$ are the target of development for cooling the nuclear components of an ADS, like the blanket and the target. Most experimental data on temperature profiles for liquid metals are going back to the Fast Breeder Reactor (FBR) development. A reformulation of such data in universal variables $T^+=f(y^+)$ is given in [Kad81] and for lower Pr e.g. in [Fuc73]. The large thermal conductivity causes very thick thermal boundary layers so that the logarithmic region, which in liquid metals begins at $y^+ Pr$ = 1, starts for $Pr = 0.025$ at y^+=400, Fig. 3-3. At small Reynolds numbers a logarithmic region may even not exist because the conductive thermal boundary layer may reach the centre of the channel. The profile increases continuously in the complete channel. Thus, the gradient of T^+ is not only important near the wall, but also in the core of the flow. As the temperature profile is very much different from the velocity profile (which is only similar to the temperature profile at $Pr = 0.7$), we get Pr_t data which are not constant over y^+, see Fig. 3-4 from DNS by [Kaw99]. This means that the formulation for the spatial distribution of Pr_t has to be accurate in the complete channel, whereas the more important area is again the near wall range. – At these Prandtl numbers a high Peclet number formulation of the temperature equation can be avoided for most Reynolds numbers of technical interest, because it is usually possible to resolve the thick conductive thermal boundary layers by the grid.

At very low Prandtl numbers and low Peclet numbers, where $Pe = Re * Pr$, the thermal conduction gets more and more dominant over the turbulent or convective heat flux. Thus, one has to clarify whether at small Pe really a detailed formula for the spatial distribution of Pr_t is required. Indeed, the experimental data by [Fuc73] and the combined LES/DNS data by [Grö81] show for the Prandtl number of sodium, Pr=0.007, that the ratio of ε_h / a is for a fixed position in the channel at Re of about 10^5 around 1 and decreases far below 1 for smaller Re, Fig. 3-5. This means, the turbulent eddy conductivity is small compared to the molecular thermal diffusivity a, and thus turbulence gives only a small contribution to heat conduction.

From this dependence one can understand that there are really parameter ranges in which calculations perform better by neglecting the turbulent heat flux model, or by setting Pr_t to infinity instead of using strange Pr_t concepts, but with increasing Peclet numbers, space dependent formulations may be required. - For the Prandtl number of mercury or lead bismuth, Pr=0.0214, ε_h / a takes values between 1 and 10 for Re around 25,000. Thus, the turbulent heat flux model gets important and an adequate local Pr_t formula is required. And for the Prandtl number of air, Pr=0.7, ε_h / a takes values of 30 and larger, which means, the turbulent heat flux model is transporting nearly the complete heat and the contribution by conduction is of minor importance. Therefore, when the conductive wall layers are resolved, the quality of the results is almost entirely determined by the adequacy of the local Pr_t formula.

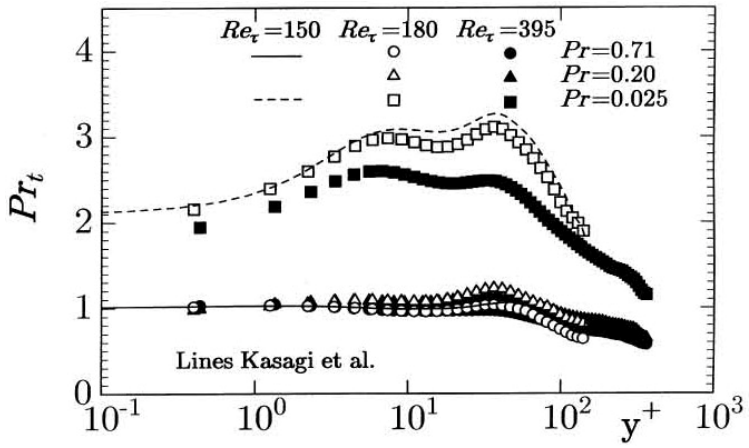

Fig. 3-4 DNS results for the turbulent Prandtl number for Pr=0.7, 0.2, and 0.025 [Kaw99].

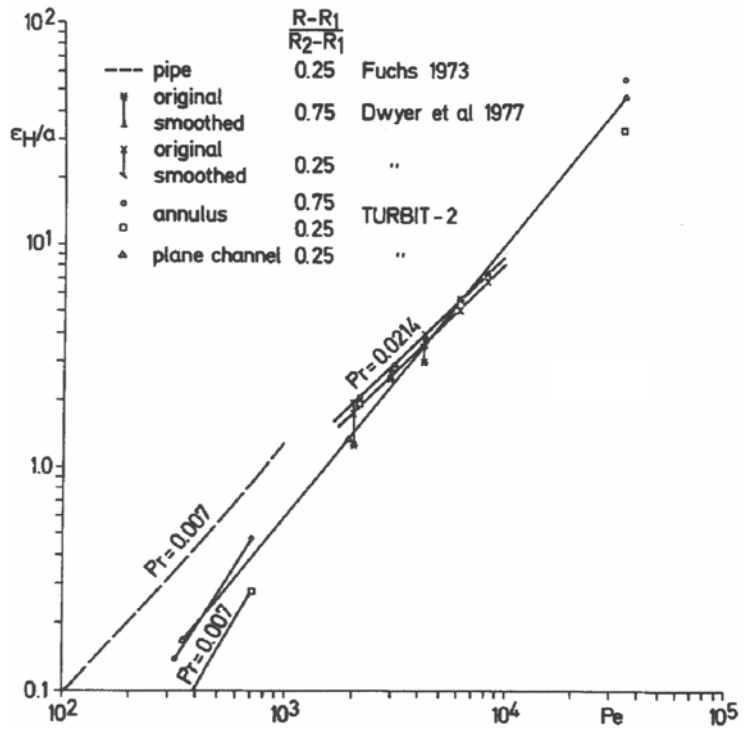

Fig. 3-5 ε_h / a dependent on Pe for y/D=0.25 [Grö81].

This assessment means, at very low molecular Prandtl numbers, like for sodium, and at low Reynolds numbers a qualitatively accurate, but not a quantitatively accurate Pr_t formula may

be sufficient, but with increasing Reynolds number and with slightly increasing Prandtl number, e.g. at that one for heavy liquid metals, we are in a transition range where the value of Pr_t becomes more and more important, and at Prandtl numbers around one the Pr_t formula governs in all low Reynolds number formulations completely the numerical temperature results. Therefore, in most applications an accurate formulation for the spatial distribution of Pr_t is essential, especially in the near wall area. And in applications using high Peclet number formulations at Prandtl numbers from 0.02 to about 1 the formula has in addition to be consistent with the applied wall functions to avoid unphysical dependence on the numerical grid.

3.2.6 Turbulent Prandtl number concept in buoyant flows

The discussion of the behaviour of the eddy conductivity approach and of the turbulent Prandtl number concept, when it is applied to buoyant flows like RBC and IHL, is based on data from our DNS for horizontal fluid layers.

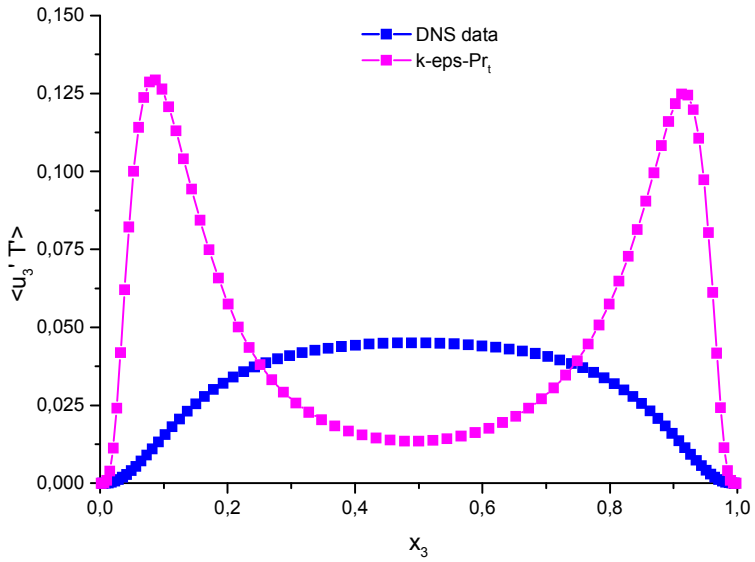

Fig. 3-6 DNS data for the vertical distribution of turbulent heat flux $\overline{u_3'\theta}$ and for its prediction by a k-ε-Pr_t model for RBC, Ra=10^5 and Pr=0.025 [Oti03].

In Rayleigh-Bénard convection the turbulent heat flux is directed upward and more or less constant in the core of the fluid layer, Fig. 3-6. Here, for the moderate Ra and low Pr, the thermal boundary layers are rather thick. The DNS results for a k-ε-Pr_t formulation of the turbulent heat flux with the default coefficients $C_\mu = 0.09$ and $\mathrm{Pr}_t = 0.9$ are qualitatively quite different [Oti03]: They show strong peaks in the conductive wall layers and a minimum in the middle. The turbulent Prandtl number which is required to get the correct results could be analysed by the ratio of the two given fluxes: It has to be much larger than one near the walls to reduce there the turbulent heat flux, and it has to be much smaller than one in the middle to increase there the heat flux. The problem gets even worse if fluids with Pr=0.7 are considered. There it is found that Pr_t goes down to about zero in the core of the fluid layer [Grö92]. The reason is that the fluid layer is widely isothermal in the core and thus the temperature gradient is very small or even zero so that the turbulent heat flux calculated from the gradient in eq. (3-5) has to be blown up by using a very small turbulent Prandtl number. In the wall layer, again values larger than one have to be used to correct for the over-prediction by the

large gradient. Such variations of a model coefficient between zero and large values indicate that this modelling concept completely fails for this buoyant horizontal fluid layer.

In the internally heated convection layer we have a homogeneously distributed heat source in the fluid. Most of the released heat is transported upward, as can be analysed from the thicknesses of the thermal boundary layers at the lower and upper walls, Fig. 2-4. In addition it is observed that the temperature maximum is not far away from the upper wall. Thus, we observe an extended vertical area inside the fluid layer of about 50% of the channel height over which the heat is transported towards the temperature maximum, i.e. against the temperature gradient [Grö82]. This counter-gradient heat flux occurs at all Rayleigh numbers for which we performed simulations up to now [Wör97]. Thus, any modelling of the turbulent heat flux based on gradient assumptions including the turbulent Prandtl number concept will fail to predict adequate temperature profiles in internally heated fluid layers. This complete failure of the method has also been found in practical applications of CFD codes to investigations of the IHL [Din97].

As problems with buoyant flows are manifold, there were already investigations of adapting mixing length models to buoyancy influenced flows, and on transferring these adaptations to turbulent Prandtl number formula, see references in [Rodi93]. There was also intensive work on investigating the applicability of the different classes of turbulence models on buoyant convection, see e.g. the review in [Han02]. From those and from our own investigations it has to be concluded that turbulent Prandtl number formula which are known from other flow types, like from forced convection in channels, cannot be applied to purely buoyant flows, because the complete modelling concept has serious principal deficiencies. It is going beyond the subject and extent of this report to discuss the reasons for this. An access to explanations can be found in [Han02] and in [Wör98].

These deficiencies of the turbulent Prandtl number concept mean, when our current commercial CFD codes are applied to buoyancy influenced or buoyancy governed flows one should always be aware of the rather limited validity of the crude turbulent heat flux modelling which is available in the code. Much better models are required for such applications. Indeed, models with improved capabilities are available in literature; this we will discuss next.

3.3 Other turbulent heat flux models

In the following we will discuss examples for classes of turbulent heat flux models which do not make use of the turbulent Prandtl number concept, which account for the anisotropy of the heat flux, for the influence of varying molecular Prandtl number, and for the influence of buoyancy contributions.

3.3.1 Anisotropic first order heat flux models

Among the first order or gradient models the 2+2 or 4-equation models should be suitable for a wide range of molecular Prandtl numbers, because they introduce separate time scales for the velocity field, k/ε, and for the temperature field, $\overline{\theta^2}/\varepsilon_\theta$. Variants which are in some terms adapted to the requirements of variable Prandtl number flows are provided e.g. in [Nag88] using mixed time scales and in [Nag94] using hybrid time scale formulations. The

mixed time scale model is investigated in [Oti07] in its tensorial form as proposed by Daly and Harlow [Dal70] which allows for better anisotropic transport features as this is expected to be relevant in flows with strong field forces:

$$\overline{u_i'\theta} = -C_{k\theta}\sqrt{\frac{k}{\varepsilon}\frac{\overline{\theta^2}}{\varepsilon_\theta}}\,\overline{u_i'u_j'}\,\frac{\partial \overline{T}}{\partial x_j} \tag{3.14}$$

Here, $C_{k\theta}$ =0.4 is the model coefficient for the mixed time scale model. In RBC with *j=3* pointing in the vertical direction, this reduces to:

$$\overline{u_3'\theta} = -C_{k\theta}\sqrt{\frac{k}{\varepsilon}\frac{\overline{\theta^2}}{\varepsilon_\theta}}\,\overline{u_3'^2}\,\frac{\partial \overline{T}}{\partial x_3} \tag{3.15}$$

The vertical turbulent heat flux is physically strongly coupled to the vertical velocity fluctuation. Accordingly, in this modified Daly and Harlow model, which is the first term of the AHM model discussed below, the heat flux depends explicitly on this quantity. On the other hand, this means, we need a modelling for twice the kinetic energy of the vertical velocity fluctuation $\overline{u_3'^2}$. This could be achieved by assuming isotropy and calculating it from k , but for buoyant flows it would be more accurate to approximate it either by an ASM approximation or by a separate transport equation. The behavior of this 4 or 5-equation model in RBC is considerably better than that of the turbulent Prandtl number concept, Fig. 3-7. Using the mixed time scale is clearly preferable over using the time scale only of the velocity or temperature field. Nevertheless, for this purely buoyant convection the model (3.15) is still not sufficient, because it is exclusively governed by a gradient assumption.

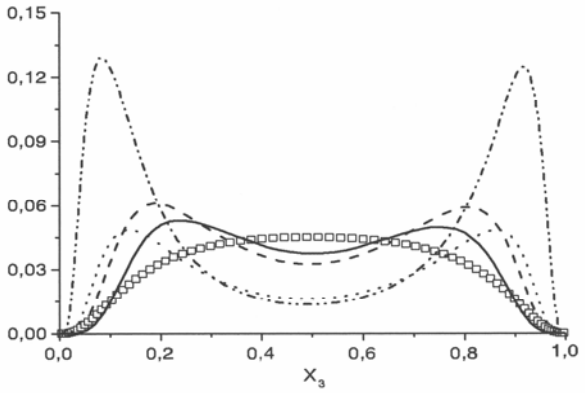

Fig. 3-7 DNS data for the vertical distribution of turbulent heat flux (-□-), for its prediction by a k - ε - Pr_t model (-··-), by eq. (3.15) (- - -), by (3.15) with velocity time scale (···), and by (3.15) with temperature time scale (—) for RBC, Ra=10^5 and Pr=0.025 [Oti07].

In the transport equations for the temperature variance $\overline{\theta^2}$ (3.3) and for its dissipation ε_θ also some closure terms appear. Examples of our DNS analyses or model proposals for these terms were published for RBC in [Grö92], [Wör95], [Wör99], [Oti03], [Oti05].

3.3.2 AHM-type models

The Algebraic Heat flux Models introduce additional terms which help to get rid of the dominance of the gradient assumptions which hinders good modelling in all those convection types in which gradients become approximately zero like in RBC. RANS models of this type

were deduced in [Mer76], [Gib78], [Lau88], or [Han02]. In starting from the transport equations for the turbulent heat fluxes, assuming fully developed flow and assuming local equilibrium the latter author deduced the following algebraic heat flux model, in which the mixed time scales are in addition implemented as in [Oti07]:

$$\overline{u_i'\theta} = -\sqrt{\frac{k}{\varepsilon}\frac{\overline{\theta^2}}{\varepsilon_\theta}}\left[C_1\overline{u_i'u_j'}\frac{\partial\overline{T}}{\partial x_j} + C_2\overline{u_j'\theta}\frac{\partial\overline{u_i}}{\partial x_j} + C_3 g_i\beta\overline{\theta^2}\right] \tag{3.16}$$

In RBC with *j=3* in the vertical direction no mean velocities exist. Thus, this reduces to:

$$\overline{u_3'\theta} = -\sqrt{\frac{k}{\varepsilon}\frac{\overline{\theta^2}}{\varepsilon_\theta}}\left[C_1\overline{u_3'^2}\frac{\partial\overline{T}}{\partial x_3} + C_3 g_3\beta\overline{\theta^2}\right] \tag{3.17}$$

In this model the vertical turbulent heat flux also depends on the vertical velocity fluctuation $\overline{u_3'^2}$, for which it is wise to solve an additional transport equation. The model in addition depends on a buoyancy term involving the temperature variance $\overline{\theta^2}$. The behavior of this algebraic 5-equation heat flux model in RBC is considerably better than that of the two discussed before, Fig. 3-8. Thus, the problems with the dominance of the temperature gradient term are fully compensated by the buoyancy term involving the temperature variance. This term follows formally from the heat flux equation where it is the buoyant production term. Comparison between Fig. 3-7 and Fig. 3-8 demonstrates that this is the key term in modeling the turbulent heat flux in buoyant flows. This model represents some anisotropic transport features by the other terms involved, and it is due to the mixed time scales applicable for a wide range of Prandtl numbers. So, it should be a promising basis for achieving better heat flux models for ADS typical applications.

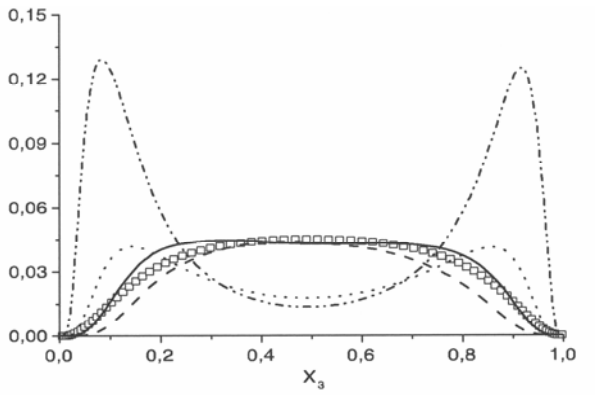

Fig. 3-8 DNS data for the vertical distribution of turbulent heat flux (-□-), for its prediction by a k-ε-Pr_t model (-··-), by the AHM model eq. (3.17) (—), by (3.17) with velocity time scale (···), and by (3.17) with temperature time scale (---) for RBC, Ra=10^5 and Pr=0.025 [Oti07].

3.3.3 Second order heat flux models

The full second order heat flux models are based on the transport equations for the turbulent heat fluxes and for the second moment of the temperature field (3.3), which is the temperature variance $\overline{\theta^2}$. These equations can be formally deduced from the momentum and energy equations, see e.g. [Don73]. Of course, there a large number of closure terms appear again. Modelled forms of these equations are discussed e.g. in [Don73], [Lau89], [Rodi93], and with the focus on liquid metal heat transfer modelling in [Car97]. The latter model, called

the Turbulence Model for Buoyant Flows (TMBF), was developed to get in a first step for our FLUTAN code [Wil96], [Grö02] an improved treatment of the turbulent heat flux in buoyant flows in which the temperature field gives the main source for convection. The TMBF is the combination of a low Reynolds number k-ε model with a full second order heat flux modelling involving the temperature variance equation and as an option also the dissipation equation for the thermal variance. So, it uses 4 or 5 equations for modelling the heat flux vector. The modelling is in many terms adapted to liquid metal convection; some of these models are deduced from our DNS data, e.g. from [Wör95] or [Wör99]; the latest model version of the TMBF is given in [Car03].

The performance of the TMBF was compared to other models in two benchmarks, see e.g. [Bau97] and [Ari04]. In both, several participants recalculated the TEFLU experiment [Kne93], [Kne98] in which the mixing of a hot sodium jet was analysed in a highly turbulent surrounding formed by a multi jet environment. The TMBF results for the axial development of the radial temperature profile in the jet clearly profit from the anisotropic heat flux modelling compared to the isotropic k-ε-Pr_t modelling in which the radial heat flux in this non-buoyant case is overestimated, Fig. 3-9. For the buoyancy influenced cases the TMBF results were also superior to any other modelling, independent on which Pr_t -formula was used, but nevertheless the TMBF still needs further improvements [Car03]. One reason could be, that the used k-ε model applies the standard model for turbulent k-diffusion and does not include special buoyancy extensions as discussed in chapter 2.3. Another reason could be that the k-ε model is an isotropic momentum flux model which should at least be replaced by an ASM to account also for the required strong anisotropy in the momentum exchange in buoyant flows.

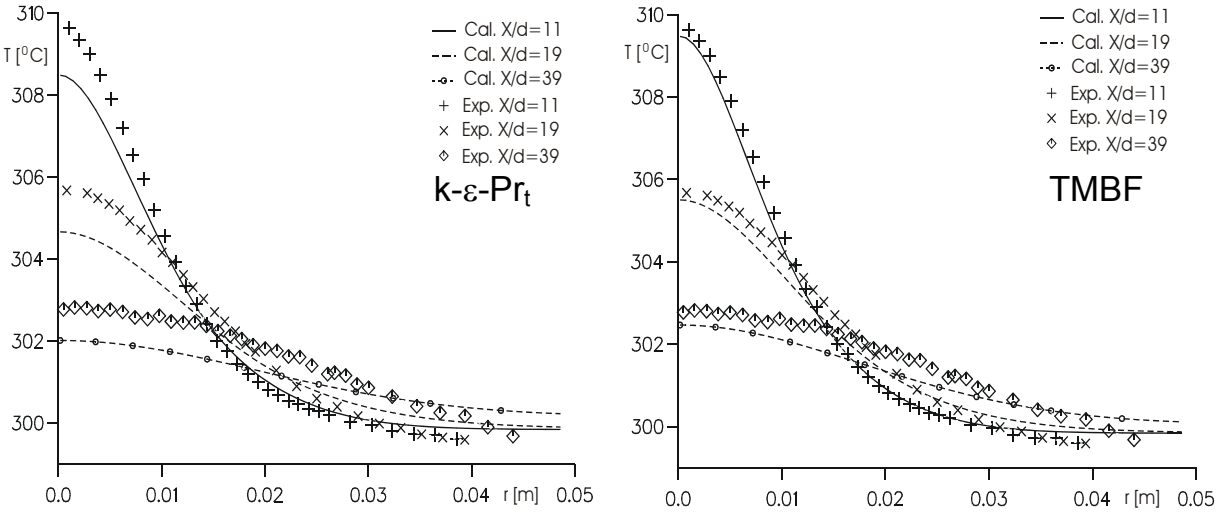

Fig. 3-9 k-ε-Pr_t and TMBF compared to TEFLU forced convection experimental results, $\mathrm{Re}_{jet}=10^4$, d= orifice diameter, x=distance to orifice [Car03].

A further advantage of a second order model is that we get the results to analyse an approximate distribution of the local turbulent Prandtl number which would be required to get the same radial heat flux with a k-ε-Pr_t model as with the TMBF. Within the computational domain, which starts at x/d=6, Pr_t takes values from below 2 at the jet axis at the lower end of the domain up to beyond 5 at the position of the maximum of the temperature gradient,

Fig. 3-10. This indicates that Pr_t shows also in jets, as expected, complicated spatial distributions. Large Pr_t values reduce the turbulent heat flux, so conduction becomes more important. Nevertheless, the other benchmark participants found no acceptable approach to get with the k-ε-Pr_t concept acceptable data for the temperature profiles which reach those of the TMBF [Ari04].

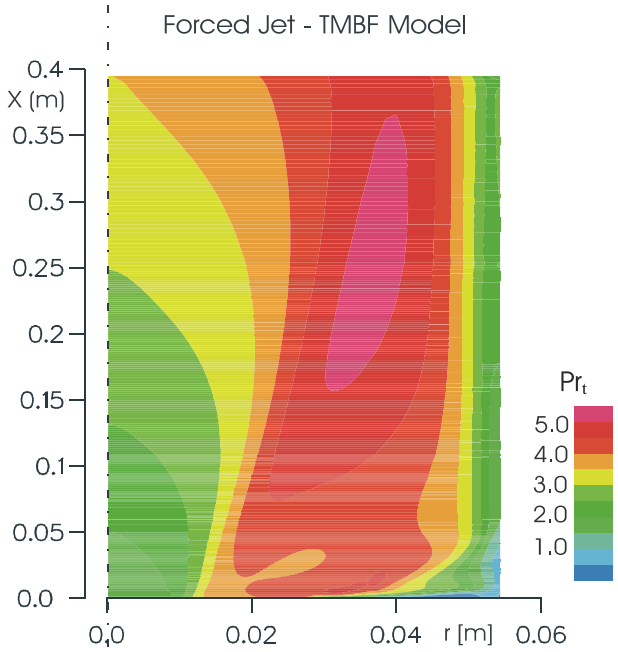

Fig. 3-10 Pr_t analyzed from the TMBF results for the TEFLU forced convection experiment, X and r=co-ordinates within computational domain, $Re_{jet}=10^4$ [Car03].

In the transport equations for the three turbulent heat fluxes $\overline{u_i'\theta}$ also some closure terms appear. Examples of our DNS analyses with different molecular Prandtl numbers or model proposals for these terms were published for RBC in [Wör93], [Wör95a], [Wör99], [Oti03], [Oti05a], for IHL in [Grö82], [Wör97], [Cha07a] and for liquid metal forced convection in [Grö87]. Meanwhile, some of our earlier model proposals are not only successfully applied in our FLUTAN code, but also by other authors in their codes; see e.g. [Ken04], who found it necessary to implement the molecular destruction model of [Wör95a] to get accurate simulation results for magnetically controlled convection. This demonstrates that the proposed models are not only of academic relevance, but also of practical relevance in CFD applications.

4 Proposal for an improved turbulence modelling

4.1 Modelling targets

In chapter 2 and 3 we learned about the fundamental and practical deficiencies of those RANS turbulence models which are used in current commercial CFD codes, we learned about the physical requirements which should be fulfilled by the models, and we noticed, that there exist better models or special model contributions, many of which are proven successful against DNS data, and some of which are already proven successful in CFD applications.

Thus, there are clear indications that the known models could indeed help to improve the situation for ADS typical single-phase flow simulations if they would become available in commercial CFD codes. So, we will try in the following to give a rough sketch of a numerically efficient RANS model which should allow for considerably improved and more reliable investigations of such flows.

The geometric flow conditions which have to be covered by the physical modelling should account for ADS-typical application fields: We need models to investigate the momentum and heat transfer in channels with very different geometries, ranging from large pipes, down to the very narrow subchannels in fuel subassemblies. On the other hand we have also to investigate the flow and mixing in large inlet and outlet plena, or the buoyant heat removal from large fluid pools. The models are needed from small velocities, respectively Reynolds numbers, with laminar flow up to large velocities or large Reynolds numbers (Re=10^5 to 10^6) with turbulent flow. The fluids which have to be considered cover a wide range of Prandtl numbers, from light liquid metals (Pr=0.006) over heavy liquid metals (Pr=0.025) and air (Pr=0.7) and hot water (Pr≈1) to organic fluids (Pr=10…100…). The involved flow types in all these channels are forced convection specified by pressure differences or volumetric flow rates, purely buoyant convection driven by density differences due to heating and cooling, and mixed flow conditions with any orientation of the mean flow vector against the gravity vector.

Among the physical phenomena or effects which are needed in the turbulence models is the strong anisotropic mass, momentum and heat transfer. This becomes important when gradients in the spanwise direction exist in the mean fields. It occurs in nearly all ADS-typical applications, either in the near-wall area or due to buoyancy everywhere in the fluid domain. The influence of buoyancy has to be treated consistently throughout the complete turbulence model. It may become important in turbulence models where it is not expected from a first look at the problem, but where the investigation of the transport equation for a closure term may show that there really occurs a formal dependence on buoyancy parameters. Time scales of turbulent fluctuations often occur explicitly or implicitly in turbulence models. The corresponding modelling has to be done carefully because in the wide Prandtl number range the timescales in the velocity and in the temperature field may be very different.

In choosing the modelling concept we have to consider that there are many flows in which the gradients of the mean velocity and temperature fields vanish over wide areas, but nevertheless there is a considerable turbulent transport of the corresponding quantity, or the gradients are locally or over wide areas opposing the momentum or heat fluxes. Thus we should avoid models which dominantly depend on gradients of the mean fields. Regarding the turbulent heat transfer modelling we should apply a degree of sophistication which is consistent to that of the turbulent shear stress modelling. This is especially true when buoyancy is involved because the temperature field contributes in such cases to the driving forces which should therefore be more accurate as it is usually accepted in forced flows. Thus, we have to refrain from applying the turbulent Prandtl number concept to determine the turbulent heat fluxes.

Regarding the numerical efficiency of the model one should not add too many additional equations so that the numerical effort is not strongly increasing. Nowadays, the 2-equation models for the turbulent momentum transfer are well accepted by engineers and are consid-

ered as a standard. So, on the heat transfer side one should try to reach the mentioned objectives with a model type requiring a similar effort, which means with a model which uses not more than two further equations. Engineers usually have a lot of experience in using their common tools and behave therefore often quite conservative when new modelling is offered; so, a more detailed heat flux modelling should be combined with the well known and well accepted modelling for the shear stresses. Finally, the modelling should be numerically robust so that the numerical effort is roughly predictable and the treatment of occasionally occurring convergence problems needs no new and very specific knowledge. Such a model should reach a good acceptance not only among the users, but also among the CFD code developers and providers.

4.2 Modelling proposal

According to the experience and modelling status discussed in this report and according to the targets given above, we give the following sketch for RANS modelling of turbulent momentum and heat fluxes: For simplicity, the model concept is discussed here for *j*=3 being the vertical direction; the generalized forms of some models are given above or in the original literature.

The selection of a suitable class of models for turbulent momentum transfer from Tab. 2-1 is based on the desired abilities to simulate the anisotropic momentum transfer, to simulate flows with counter-gradient shear stresses, to keep the numerical efficiency, and to achieve acceptance. From these criteria one has to select an Algebraic Stress Model (ASM) as model basis. Such a concept involves the k-ε model. Due to accuracy reasons, especially when buoyancy influences have to be considered, this should be applied in a low-Reynolds number formulation, this means, the viscous wall layer is well resolved and additional uncertainties in the wall conditions are avoided. Of course, all formally explicitly appearing buoyancy contributions have to be included in all engaged transport equations. From the not directly obvious buoyancy contributions one should include the buoyancy extended turbulent kinetic energy diffusion by [Cha07], as it is given in the complete version in eq. (2-15), because this is required for modelling the counter-gradient turbulent energy diffusion in buoyant horizontal fluid layers. Several simplified versions of this model are given e.g. in [Cha05]. The model in eq. (2-15) contains additional closure terms: The triple correlations $\overline{u_3'^3}$ and $\overline{u_3'\theta^2}$ can be calculated using models by Launder [Lau89] and by Otić et al. [Oti05], respectively. The third term, $\overline{u_3'^2}$, could be provided by the ASM itself, but as this term is essential in buoyant flows and as it is needed also in other model parts below, it should be considered to calculate it with higher accuracy and not bound to local information only. This means it should be calculated by an additional modelled transport equation e.g. as in Launder et al. [Lau75] and extending their equation to buoyant flows, or similar to the equation as in Durbin [Dur95]. Of course, the simpler and more general treatment would be to calculate all velocity fluctuation variances from the ASM approach, because then one would not need to select two coordinate directions horizontally and to distinguish in the modelling between the direction in which the gravity acts and in which the gravity component is zero.

The selection of a suitable model class for turbulent heat transfer from Tab. 3-1 is based on the desired abilities to simulate the anisotropic heat fluxes, to simulate flows with extended areas with zero-gradient or counter-gradient heat fluxes, to keep the additional numerical

effort small, and to achieve acceptance. From these criteria one has to select an Algebraic Heat flux Model (AHM) as model basis. Such a concept involves for buoyant flows the transport equation (3.3) for the temperature variance $\overline{\theta^2}$. To avoid the application of empiric values for the very critical time scale ratio R as defined in (3.4), which is often applied in modeling the sink term ε_θ in this equation, a separate transport equation should be solved for this dissipation of the temperature variance, especially when fluids with $Pr \neq 1$ are engaged. For $Pr \neq 1$ anyway both transport equations are required, even in the non-buoyant case, because the time scales k/ε in the momentum field and $\overline{\theta^2}/\varepsilon_\theta$ in the thermal energy field are different and therefore it is quite common to apply the mixed or combined time scale which needs all four equations. Due to accuracy reasons, especially when buoyancy influences have to be considered, this modelling concept should be realized in a low-Peclet number formulation, this means, the conductive wall layer is well resolved and additional uncertainties in the wall conditions are avoided. This is easy to be realized in liquid metal flows because these obey very thick conductive wall layers, but it may not be practicable in high Peclet number flows at Pr>>1.

The AHM formulation could be based on the algebraic formulation with the mixed time scales as given in eq. (3.16) according to [Oti07]. The modelling in the transport equations for $\overline{\theta^2}$ and ε_θ could follow the approach as in the TMBF model [Car03], which contains already a number of extensions for variable Prandtl numbers, but which still needs improvement. Thus, the improved turbulent diffusion modelling should be applied as given in [Oti05]. Regarding the calculation of the variance of the vertical velocity fluctuation $\overline{u_3'^2}$, the same holds as just discussed with the momentum transfer model: A separate transport equation would allow for more accurate results, but makes the application to cases complicated in which the channel is tilted against the gravity vector. So, from the numerical effort and generality, the pure ASM approach to determine $\overline{u_3'^2}$ might be of practical advantage.

The total turbulence model resulting from this proposal is a 4-equation or 5-equation ASM+AHM model which does not involve any turbulent Prandtl number for heat and which avoids any explicit assumption for the problematic ratio R of the thermal to mechanical turbulent time scales. It obviously meets all requirements which were formulated in chapter 4.1. So, we do not need necessarily a full second order approach to simulate buoyancy influenced or even buoyancy driven flows as it is formulated in the Best Practice Guidelines [Cas00].

4.3 Modelling procedure

Of course, one could just realize right now the model concept given in chapter 4.2 and investigate its performance in a CFD code. Nevertheless one should keep in mind, that some of the model components have only been deduced and validated for buoyant horizontal fluid layers, and that there are still some variants which may be as useful or even better as those mentioned in the proposal. E.g., instead of starting from the AHM approach given in eq. (3.16) one could also start from an AHM approach as given in [Han02] and introduce there the mixed time scale and the molecular heat flux destruction term as developed in [Wör95a] which was found inevitable in simulations by [Ken04]. Or, one has still to clarify whether it is really necessary to solve a fifth transport equation, i.e. for $\overline{u_3'^2}$, or whether it is sufficient to get these data just from the local ASM approach. Thus, some further a-priori investigations could

be performed in advance. Additional examples are the performance of the model components in buoyant flows at higher Rayleigh numbers, in mixed flows and in forced flows; the behaviour in channel flows and in large containers or pools; and the behaviour in a wider range of Reynolds numbers and Prandtl numbers. In all these investigations also a more detailed determination of the model coefficients could be performed. The required DNS data can in parts be taken from our results provided in the database by [Wör97a], by the recent data by [Oti05] and [Cha05], and from literature. There are e.g. excellent data bases from DNS by Kawamura [Kaw07], by Kasagi [Kas07], by Nagano [Nag07] and others, or with well validated experimental and numerical data gathered by teams under the ERCOFATC header [ERC07].

One of the following steps will be to select a CFD code as working horse for implementation. In a code which has a non-linear first order shear stress model, the implementation could be performed in two steps: In a first step one implements the AHM heat flux model with its 2 or 3 additional equations. In combining this in an interim step either with one of the non-linear shear stress models which have some limited anisotropic transport features, or in case of Star-CD with the V2F model by [Dur95], or even with the full second order shear stress model, one could roughly adapt, validate and investigate the performance of this heat flux model. And in the second step one would also implement the ASM model for the shear stresses.

The adaptation and optimization of the model coefficients of the complete model is done by applications to specific fundamental flows and to common benchmark problems. It may be necessary that one has not only to optimize the new coefficients, but perhaps also the already well-known coefficients in standard parts of the model may need reconsideration. Next, the complete model can be validated by applications to other fundamental flows, e.g. as in [Ties98], and to common benchmark problems. In this phase it will turn out whether the proposed model indeed shows all the features in the desired manner as it was formulated in chapter 4.1. Finally the model and the code should be ready for practical engineering tasks.

5 Conclusions

In numerical investigations of turbulent heat transfer in nuclear components, e.g. in ADS systems, we need physical models which are not quite common. In the past we already had in the nuclear community suitably extended models available in our codes, but meanwhile the effort of keeping track with commercial codes is too large so that many institutions shifted from CFD codes developed in the nuclear community to commercial CFD codes. As a consequence we have to consider what the abilities of the large commercial codes are and what our necessities are from the physical side. As there is no reliable and accurate prediction of the temperature field without accurate prediction of the velocity field, one has to start with considering the turbulent shear stress modelling.

The turbulent momentum flux models are classified and discussed in the light of their ability to reproduce flows e.g. with counter-gradient fluxes, with strong anisotropic momentum fluxes, and with strong influence by buoyancy forces. In the commercial codes we find models which could treat the first two peculiarities quite well, but mostly at some numerical ex-

pense. By investigating the physical needs for the models from experimental and numerical results from more than 20 to 40 years ago one finds, that nearly all technical flows, especially fuel bundle flows, show a strong anisotropy of the momentum and heat exchange in the near wall range and that sufficient numerical results can only be achieved by an adequate anisotropic shear stress modelling. Within the last 5 to 10 years this knowledge was just reproduced by applying commercial codes to fuel bundle flows: It is found that the isotropic k-ε model is insufficient for bundle flows, that specially adapted non-linear models do better, and that full second order models could still be improved. Here we discussed, that this anisotropic momentum transfer is important very close to walls, this means when a low-Reynolds number formulation of the turbulence model is applied, and that it is less important when a high-Reynolds number formulation is used. This relevance is also found with similar importance in bubbly flows.

The flow in the narrow channels of fuel assemblies shows at small pitch to diameter ratios P/D regular cross flow patterns which cause intensive inter-channel mixing. The adequate tools to simulate such flows could hardly be specified in advance. It was already shown that steady RANS calculations fail to predict adequate mixing data, whereas LES can predict this mixing phenomenon as it occurs in such flows, but the numerical effort of LES is too large for systematic flow investigations. In considering the time averaging which is immanent to the RANS method, in estimating from two-point correlations a time window which is required for averaging, and in investigating the frequencies which are caused by the transport of the vortex patterns found in experiments one could conclude that unsteady RANS, so called URANS, could reproduce these features of the flow. And indeed, this was recently practically shown. So, in going back to the definition of the variables in which a code is calculating, one could also in this case quite well decide in advance what the adequate method for a simulation would be. The definition of the variables is also important for the interpretation of the experimental and numerical results, because these might use quite different definitions, e.g. long-time averaging in experiment and ensemble averaging in URANS. Both lead to very different results for the turbulence data.

The influence of buoyancy is investigated on the basis of our DNS data for horizontal fluid layers. It is well known that buoyancy is insufficiently treated in the commercial codes. With analyses of our data we can show that one reason comes from the crude modeling used for the turbulent heat fluxes, the other one comes from the fact, that there are buoyancy influences hidden in closure terms which can only be detected in investigating their transport equations. An extended model for the turbulent diffusion of the kinetic turbulence energy was given which improves considerably the predictability for buoyant horizontal fluid layers. Thus, a considerable improvement of the extended k-ε model could be expected for buoyant flows. The modeling of the always buoyant bubbly flows is a much more serious problem and needs still further investigations and development for all closure terms in the k-equation.

The turbulent heat flux models are classified and discussed in the light of their ability to reproduce flows e.g. with counter-gradient heat fluxes, with strong anisotropic fluxes, and with strong influences by buoyancy forces. In the commercial codes we find no specific heat flux model at all, except for the turbulent Prandtl number concept, which assumes Reynolds analogy between momentum and heat transfer, in which the proportionality factor is the turbulent Prandtl number. This is usually assumed to be constant. Thus, we find in the commer-

cial codes a serious imbalance between options with a highly sophisticated modelling of the turbulent momentum transfer applying a large number of transport equations for turbulence quantities, but on the scalar transport side we have only the modelling by using one number, the turbulent Prandtl number. Most code users are aware of the problem with this number, but unfortunately they apply the constant default value given in the code.

Here we developed a simple model for the local turbulent Prandtl number as given in eq. (3-12) which holds for stationary and fully developed channel flows like in pipes, plane channels, annuli, or in fuel bundles. It holds for smooth and rough walls, and for all types of thermal wall conditions like symmetric and asymmetric cooling and heating. It can be applied at all wall distances, for all Reynolds numbers with turbulent flows, and for all Prandtl numbers with $Pr \geq 0.02$. A simplified version of this exists already in literature and is validated there by using radial profiles of the turbulent Prandtl number data and by recalculated universal temperature profiles. Validations which only apply integral data like Nusselt numbers are not sufficient to ensure a correct radial distribution of thermal data. The relevance of the locally formulated turbulent Prandtl number heavily depends on the molecular Prandtl number of the fluid and on the type of wall modeling. For $Pr \geq 1$ and a low-Peclet number heat flux modeling, that means, the conductive sublayer is spatially resolved, it is shown that an accurate formulation of the turbulent Prandtl number is of utmost importance within the first y^+ values, whereas in a high-Peclet number formulation, i.e. when the conductive sublayer is not resolved, the turbulent Prandtl number has practically no or only a weak influence because the calculated temperature profile is mainly determined by the thermal wall function. To avoid unphysical dependence on the grid, especially at $Pr \approx 1$, one has to use consistent formulations in the turbulent Prandtl number approach and in the wall functions. The correlation developed here is consistent with the standard wall functions so far as the Kader-correlations for T^+ are applied in the codes. With decreasing molecular Prandtl number, the influence of the size of the turbulent Prandtl number is decreasing, but not of its local variation; it still needs adequate modeling throughout the complete channel width. This holds down to the Prandtl number of light liquid metals at large Reynolds numbers, at which the heat is transferred at about equal amounts by conduction and by turbulent convection. Only for the Prandtl number of sodium and at lowest Reynolds numbers most heat is transported by conduction so that the quality of a space-dependent turbulent Prandtl number may be considered less important. For reactor applications one can state that in all flows a space dependent formulation is required. This conclusion, which is deduced from physical arguments, is consistent with the practical findings in many code and model benchmark calculations.

Turbulent Prandtl number models for fully developed flow exist in large number in literature, but there is only one which is sometimes applied which does not depend on wall distance, but on local turbulence data, so that it could be applied e.g. to mixing layers. Investigating the turbulent Prandtl number concept for buoyant convection shows that the concept completely fails. Thus, a more sophisticated modeling is required in the commercial codes to include the strong anisotropy in buoyant flows and to treat the heat flux through the often occurring wide regions with zero temperature gradient, or even opposing temperature gradient.

Among the more sophisticated heat flux models, in the class of first order 4-equation models one model was given in a tensorial form to account for some anisotropy as it occurs due to the buoyancy force; some models account quite well for the influence of variable Prandtl

number, but these are still gradient models. They perform better than the turbulent Prandtl number concept, but are still not sufficiently accurate for liquid metal nuclear applications. Algebraic heat flux models with mixed time scales were found to have promising behavior in horizontal fluid layers, because they contain additional terms which could compensate for the wrong counter-gradient heat flux predictions of a simple gradient flux model. A full second order heat flux model, which contains a number of DNS data based model extensions, was investigated in practical CFD applications for the mixing of a hot sodium jet. In different benchmarks the model was found to be superior to the turbulent Prandtl number concept and that it predicts well the anisotropic turbulent heat flux in the jet.

A modelling concept is proposed which is based on the physical requirements for ADS typical CFD applications and on the abilities of the different models as outlined in the discussions. The proposed turbulence model for momentum and heat transfer is a 4-equation or 5-equation Algebraic Shear stress Model (ASM) combined with an Algebraic Heat flux Model (AHM) which does not involve any turbulent Prandtl number for heat transfer and which avoids any explicit assumption for the problematic ratio R of the thermal to mechanical turbulent time scales. It should have the ability to treat flows in a wide range of Reynolds and Prandtl numbers, to include the important anisotropic transport mechanisms for momentum and heat; it offers the ability to predict fluxes in areas with zero or opposing gradients of the mean fields, and to model consistently the influence of buoyancy forces. The accuracy of predictions with such a RANS turbulence model should be considerably improved compared to the accuracy of the models which are currently available in the market dominating commercial codes. A quantification of the accuracy increase can only be given after implementation in the code and practical applications, which both are not yet available. Such a model should not only be of interest for ADS investigations, it should be of interest for any application in which buoyancy is involved, at any Prandtl number of the fluid.

6 References

[ANS07] ANSYS-CFX,
Solver Theory.
ANSYS Inc. 2007

[Ari04] Arien, B.,
ASCHLIM: A 5th FP project for the assessment of CFD codes applied to heavy liquid metals.
European Commission 2004

[Bag03] Baglietto, E., Ninokata, H.,
Turbulence models evaluation for heat transfer simulation in tight lattice fuel bundles.
Proc. of the 10th International Topical Meeting on Nuclear Reactor Thermal Hydraulics, NURETH-10, Seoul, Korea, October 5-9, 2003, paper E214

[Bag07] Baglietto, E., Ninokata, H.,
Improved turbulence modelling for performance evaluation of novel fuel designs.
Nucl. Technology 158, 2007, pp. 237-248

[Bau01] Bauer, G.S., Salvatores, M., Heusener, G.,
MEGAPIE, a 1 MW pilot experiment for a liquid metal spallation target.
J. Nucl. Mat. 296, 2001, pp. 17-33

[Bau97] Baumann, W., Carteciano, L., Weinberg, D.,
Thermal propagation effects in a vertical turbulent flow behind a jet block - A benchmark exercise.
J. Hyd. Res. 35, 1997, pp. 843-864

[Ben07] Benamati, G., Foletti, C., Forgione, N., Oriolo, F., Scaddozzo, G., Tarantino, M.,
Experimental study on gas-injection enhanced circulation performed with the CIRCE facility.
Nucl. Engng. Des. 237, 2007, pp. 768-777

[Bie96] Biemüller, M., Meyer, L., Rehme, K.,
Large eddy simulation and measurement of the structure of turbulence in two rectangular channels connected by a gap.
Engng. Turbulence Modelling and Experiments 3, Ed. W. Rodi, G. Bergeles, Elsevier 1996, pp. 249-258

[Bob85] Bobkov, V. P.,
Anisotropic turbulent heat transfer in channels of nuclear power reactors.
Translated by Plenum Publ. Corp. 1986 from Atomnaya Energiya 59, 1985, pp. 330-335

[Bun98] Bunk, M., Wörner, M.,
Direkte numerische Simulation turbulenter Rayleigh-Bénard-Konvektion in Quecksilber.
FZKA 5915, Forschungszentrum Karlsruhe 1998

[Car03] Carteciano, L., Grötzbach, G.,
Validation of turbulence models for a free hot sodium jet with different buoyancy flow regimes using the computer code FLUTAN.
FZKA 6600, Forschungszentrum Karlsruhe 2003

[Car97] Carteciano, L.N., Weinberg, D., Müller, U.,
Development and analysis of a turbulence model for buoyant flows.
4th World Conference on Experimental Heat Transfer, Fluid Mechanics and Thermodynamics. Bruxelles, June 2-6, 1997, Vol. 3, pp. 1339-1347, Pisa : Edizioni ETS, 1997

[Cas00] Casey, M., Wintergerste, T. (Eds.),
Best Practice Guidelines.
ERCOFTAC Special Interest Group on Quality and Trust in Industrial CFD, Vers. 1.0, January 2000

[Ceb73] Cebeci, T.,
A model for eddy conductivity and turbulent Prandtl number.
J. Heat Transfer 95, 1973, pp. 227-234

[Cha05] Chandra, L.,
A model for the turbulent diffusion of turbulent kinetic energy in natural convection.
Dissertation, Univ. Karlsruhe, FZKA 7158, Forschungszentrum Karlsruhe 2005

[Cha07] Chandra, L., Grötzbach, G.,
Analysis and modeling of the turbulent diffusion of turbulent kinetic energy in natural convection.
Flow, Turbulence and Combustion 79, 2007, pp. 133-154.
DOI:10.1007/s10494-007-9076-4

[Cha07a] Chandra, L., Grötzbach, G.,
Analysis and modelling of the turbulent diffusion of turbulent heat fluxes in natural convection.
5th International Symposium on Turbulence and Shear Flow Phenomena TSFP-5, Garching, Germany, Aug. 27 – 29, 2007, Proc. on CD-ROM, Ed. R. Friedrich, N.A. Adams, J.K. Eaton, J.A.C. Humphrey, N. Kasagi, M.A. Leschziner, Vol. 2, pp. 487-492, Garching : TU München
invited to appear in Int. J. Heat Fluid Flow 2008

[ChaT04] Chang, D., Tavoularis, S.,
Identification of coherent structures in axial flow in a rectangular channel containing a rod.
12th annual conference of the CFD Society of Canada, CFD2004, Ottawa, ON, May 9 - 11, 2004

[Cin04] Cinotti, L., Giraud, B., Abderrahim, H.A.,
The experimental accelerator driven system (XADS) designs in the EURATOM 5th framework programme.
J. Nucl. Mat. 335, 2004, pp. 148-155

[Dal70] Daly, B. J., Harlow, F. H.,
Transport equations in turbulence.
Phys. Fluids 18, 1970, pp. 2634-2649

[Dav90] Davidson, L.,
Second-order corrections of the model to account for non-isotropic effects due to buoyancy.
Int. J. Heat Mass Transfer 33, 1990, pp. 2599-2608

[Din97] Dinh, T.N. , Nourgaliev, R.R.,
Turbulence modelling for large volumetrically heated liquid pools.
Nucl. Engng. Design 169, 1997, pp. 131-150

[Don69] Donaldson, C. duP.,
A computer study of an analytical model of boundary layer transition.
AIAA Journal 7, 1969, pp. 272-278

[Don73] Donaldson, C. duP.,
Construction of a dynamic model of the production of atmospheric turbulence and the dispersal of atmospheric pollutants.
Workshop on Micrometeorology, Ed. D. A. Haugen, Amer. Met. Society 1973, pp. 313-392

[Dri56] van Driest, E.R.,
On turbulent flow near a wall.
J. Aeronaut. Sc. 23, 1956, pp. 1007-1011

[Dur95] Durbin, P.A.,
Separated flow computations with the k-ε−v2 model.
AIAA Journal 33, 1995, pp. 659-664

[ERC07] ERCOFTAC Database.
http://ercoftac.mech.surrey.ac.uk/

[Fuc73] Fuchs, H.,
Wärmeübergang an strömendes Natrium: Theoretische und experimentelle Untersuchungen über Temperaturprofile und turbulente Temperaturschwankungen bei Rohrgeometrie.
Dissertation, ETH Zürich, EIR- Bericht Nr. 241, Würenlingen 1973

[Gib78] Gibson, M.M., Launder, B.E.,
Ground effect on pressure fluctuations in the atmospheric boundary layer.
J. Fluid Mech. 86, 1978, pp. 491-511

[Gos06] Gosset, A., Tavoularis, S.,
Laminar flow instability in a rectangular channel with a cylindrical core.
Phys. Fluids 18, 2006, 04.4108

[Grö02] Grötzbach, G., Panefresco, C., Carteciano, L.N., Dorr, B., Olbrich, W.,
Entwicklung des Rechenprogramms FLUTAN für thermo- und fluiddynamische Anwendungen.
Programm Nukleare Sicherheitsforschung, Jahresbericht 2001 Teil 1, FZKA 6741, Forschungszentrum Karlsruhe 2002, pp. 404-410

[Grö04] Grötzbach, G., Batta, A., Lefhalm, C.-H., Otić, I.,
Challenges in thermal and hydraulic analyses of ADS target systems.
6th International Topical Meeting on Nuclear Reactor Thermal Hydraulics, Operations and Safety, NUTHOS-6, Nara, J., Oct. 4-8, 2004, Atomic Energy Society of Japan, CD-ROM, paper N6P005

[Grö06] Grötzbach, G.,
Turbulence modeling issues in ADS thermal and hydraulic analyses.
Theoretical and Experimental Studies of Heavy Liquid Metal Thermal Hydraulics, Proc. of a Technical Meeting held in Karlsruhe, Germany, Oct. 28-31, 2003
IAEA-TECDOC-1520, IAEA Wien, Oct. 2006, ISBN 92-0-111806-6, ISSN 1011-4289, pp. 9-32

[Grö77] Grötzbach, G.,
Direkte numerische Simulation turbulenter Geschwindigkeits-, Druck- und Temperaturfelder bei Kanalströmungen.
Dissertation, Universität Karlsruhe, KfK 2426, Kernforschungszentrum Karlsruhe 1977, Engl. translation in US-DOE-tr-61

[Grö81] Grötzbach, G.,
Numerical simulation of turbulent temperature fluctuations in liquid metals.
Int. J. Heat Mass Transfer 24, 1981, pp. 475 490

[Grö82] Grötzbach, G.,
Direct numerical simulation of the turbulent momentum and heat transfer in an internally heated fluid layer.
Heat Transfer 1982, Ed. Grigull, U., et al., Hemisphere Publ. Corp., Washington 2, 1982, pp. 141-146

[Grö82a] Grötzbach, G.,
Direct numerical simulation of laminar and turbulent Bénard convection.
J. Fluid Mech. 119, 1982, pp. 27-53

[Grö83] Grötzbach, G.,
Spatial resolution requirements for direct numerical simulation of the Rayleigh Bénard convection.
J. Comp. Phys. 49, 1983, pp. 241-264

[Grö87] Grötzbach, G.,
Direct numerical and large eddy simulation of turbulent channel flows.
Encyclopaedia of Fluid Mechanics, Ed. N.P. Cheremisinoff, Gulf Publ., Houston 6, 1987, pp. 1337-1391

[Grö89] Grötzbach, G.,
Turbulent heat transfer in an internally heated fluid layer.
Refined Flow Modelling and Turbulence Measurements, Ed. Y. Iwasa, N. Tamai, A. Wada, Universal Academy Press Inc., Tokyo 1989, pp. 267-275

[Grö92] Grötzbach, G., Wörner, M.,
Analysis of second order transport equations by numerical simulations of turbulent convection in liquid metals.
Proc. of the 5th International Topical Meeting on Nuclear Reactor Thermal Hydraulics, NURETH-5, Salt Lake City, USA. September 21-24, 1992, American Nuclear Society, LaGrange Park, Ill., Vol. 2, 1992, pp. 358 - 365

[Grö99] Grötzbach, G., Wörner, M.,
Direct numerical and large eddy simulations in nuclear applications.
Int. J. Heat Fluid Flow 20, 1999, pp. 222 - 240

[Han02] Hanjalić, K.,
One-point closure models for buoyancy-driven turbulent flows.
Annual Review of Fluid Mechanics 34, 2002, pp. 321-347

[Han99] Hanjalić, K.,
Second-moment closures for CFD: needs and prospects.
Int. J. Comp. Fluid Dyn. 12, 1999, pp. 67-97

[Hat06] Hattori, H., Morita, A., Nagano, Y.,
Nonlinear eddy diffusivity models reflecting buoyancy effect for wall-shear flows and heat transfer.
Int. J. Heat Fluid Flow 27, 2006, pp. 671-683

[Hoo84] Hooper, J.D., Rehme, K.,
Large-scale structural effects in developed turbulent flow through closely-spaced rod arrays.
J. Fluid Mech. 145, 1984, pp. 305-337

[Ilic05] Ilić, M., Wörner, M., Cacuci, D.G.,
Investigations of liquid phase turbulence based on Direct Numerical Simulations of bubbly flows.
Proc. of the 11th International Topical Meeting on Nuclear Thermal-Hydraulics, NURETH-11, Avignon, France, October 2-6, 2005, CD-ROM paper 022

[Ilic06] Ilić, M.,
Statistical analysis of liquid phase turbulence based on direct numerical simulations of bubbly flows.
Dissertation, Universität Karlsruhe, FZKA-7199, Forschungszentrum Karlsruhe 2006

[In03] In, W.K., Oh, D.S., Chun, T.H.,
Simulation of turbulent flow in rod bundles using eddy viscosity models and the Reynolds stress model.
Proc. of the 10th International Topical Meeting on Nuclear Reactor Thermal Hydraulics, NURETH-10, Seoul, Korea, October 5-9, 2003, CD-ROM paper E213

[Jah75] Jahn, M.,
Holographische Untersuchung der freien Konvektion in einer Kernschmelze.
Dissertation, Technische Universität Hannover 1975

[Jis79] Jischa, M., Rieke, H.B.,
About the prediction of turbulent Prandtl and Schmidt numbers from modeled transport equations.
Int. J. Heat Mass Transfer 22, 1979, pp. 1547-1555

[Jis82] Jischa, M., Rieke, H.B.,
Modeling assumptions for turbulent heat transfer.
Heat Transfer 1982, Ed. Grigull, U., et al., Hemisphere Publ. Corp., Washington 3, 1982, pp. 257-262

[Kad81] Kader, B. A.,
Temperature and concentration profiles in fully turbulent boundary layers.
Int. J. Heat Mass Transfer 24, 1981, pp. 1541-1544

[Kas07] Kasagi, N.,
DNS database at Turbulence and Heat Transfer Laboratory, The University of Tokyo.
http://www.thtlab.t.u-tokyo.ac.jp/

[Kas95] Kasagi, N., Shikazono, N.,
Contribution of direct numerical simulation to understanding and modelling turbulent transport.
Proc. R. Soc. Lond. A 451, 1995, pp. 257-292

[Kat93] Kataoka, I, Serizawa, A., Besnard, D. C.,
Prediction of turbulence suppression and turbulence modeling in bubbly two-phase flow.
Nucl. Engng. Des. 141, 1993, pp. 145-158

[Kaw07] Kawamura, H.,
DNS database at Kawamura Lab.
http://murasun.me.noda.tus.ac.jp/db/

[Kaw99] Kawamura, H., Abe, H., Matsuo, Y.,
DNS of turbulent heat transfer in channel flow with respect to Reynolds and Prandtl number effects.
Int. J. Heat Fluid Flow 20, 1999, pp. 196-207

[Kay94] Kays, W. M.,
Turbulent Prandtl number - Where are we? (The 1992 Max Jakob Memorial Award Lecture).
J. Heat Transfer 116, 1994, pp. 284-295

[Ken04] Kenjeres, S., Hanjalić, K.,
Numerical simulation of magnetic control of heat transfer in thermal convection.
Int. J. Heat Fluid Flow 25, 2004, pp. 559-568

[Kne03] Knebel J.U., Cheng X., Grötzbach G., Stieglitz, R., Müller, G., Konys, J.,
Thermalhydraulic and material specific investigations into the realization of an Accelerator Driven System (ADS) to transmute minor actinides - Final report.
FZKA 6868, Forschungszentrum Karlsruhe 2003

[Kne93] Knebel, J.U.,
Experimentelle Untersuchungen in turbulenten Auftriebsstrahlen in Natrium.
Dissertation, Universität Karlsruhe, KfK 5175, Kernforschungszentrum Karlsruhe 1993

[Kne98] Knebel, J.U., Krebs, L., Müller, U., Axcell, B.P.,
Experimental investigations of a confined heated sodium jet in a co-flow.
J. Fluid Mech. 368, 1998, pp. 51-79

[Kra98] Krauss, T., Meyer, L.,
Experimental investigation of turbulent transport of momentum and energy in a heated rod bundle.
Nucl. Engng. Design 180, 1998, pp. 185-206

[Kul85] Kulacki, F.A., Richards, D.E.,
Natural convection in plane layers and cavities with volumetric energy sources.
Natural Convection - Fundamentals and Applications, Ed. S. Kakac, W. Aung, R. Viskanta, Hemisphere 1985, pp. 179-255

[Lau72] Launder, B. E., Spalding, D. B.,
Lectures in Mathematical Models of Turbulence.
Academic Press, London 1972

[Lau75] Launder, B. E., Reece, G. J., Rodi, W.,
Progress in the development of a Reynolds-stress turbulence closure.
J. Fluid Mech. 68, 1975, pp. 537-566

[Lau88] Launder, B. E.,
On the computation of convective heat transfer in complex turbulent flows.
J. Heat Transfer 110, 1988, pp. 1112-1128

[Lau89] Launder, B.E.,
Second-moment closure: Present - and future.
Int. J. Heat Fluid Flow 10, 1989, pp. 282-300

[Law77] Lawn, C.J.,
Turbulent temperature fluctuations in liquid metals.
Int. J. Heat Mass Transfer 20, 1977, pp. 1035 1044

[Lör77] Lörcher, G.,
Laser-Doppler-Messungen von Energiedichtespektren in turbulenter Kanalströmung.
Dissertation, Univ. Karlsruhe, KfK 2448, Kernforschungszentrum Karlsruhe 1977

[Men93] Menter, F.R.,
Zonal two-equation k-ω turbulence models for aerodynamic flows.
Proc. 24th Fluid Dynamics Conf., Orlando, Florida, USA, 6-9 July 1993, Paper No. AIAA 93-2906

[Mer76] Meroney, R.N.,
An algebraic stress model for stratified turbulent shear flows.
Comp. Fluids 4, 1976, pp. 93-107

[Mey94] Meyer, L., Rehme, K.,
Large-scale turbulence phenomena in compound rectangular channels.
Experimental Thermal and Fluid Science 8, 1994, pp. 286-304

[Meyd75] Meyder, R.,
Turbulent velocity and temperature distribution in the central subchannel of rod bundles.
Nucl. Engng. Design 35, 1975, pp. 181-189

[Moe89] Moeng, C.–H. and Wyngaard, J.C.,
Evaluation of turbulent transport and dissipation closures in second-order modelling.
J. Atmospheric Sc. 46, 1989, pp. 2311-2330

[Möl92] Möller, S. V.,
Single-phase turbulent mixing in rod bundles.
Experimental Thermal and Fluid Science 5, 1992, pp. 26-33

[Nag07] Nagano, Y.,
DNS database at Heat Transfer Laboratory, Nagoya Institute of Technology
http://heat.mech.nitech.ac.jp/database/DNS.html

[Nag88] Nagano, Y., Kim, C.,
A two-equation model for heat transport in wall turbulent shear flows.
J. Heat Transfer 110, 1988, pp. 583-589

[Nag94] Nagano, Y., Shimada, M., Youssef, M. S.,
Progress in the development of a two-equation heat transfer model based on DNS databases.
Proc. Int. Symposium on Turbulence, Heat and Mass Transfer, Lisbon, Aug. 9-12, 1994, pp. 3.2.1-3.2.6, New York N.Y. : Begell House Inc. 1995

[NaHa73] Na, T.Y., Habib, I.S.,
Heat transfer in turbulent pipe flow based on a new mixing length model.
Appl. Sci. Res. 28, 1973, pp. 302-314

[Nik30] Nikuradse, J.,
Untersuchungen über turbulente Strömungen in nicht kreisförmigen Rohren.
Ingenieur Archiv, I. Band, 1930, pp. 306-331

[Nik32] Nikuradse, J.,
Gesetzmäßigkeiten der turbulenten Strömung in glatten Rohren.
VDI-Forschungsheft Nr. 356, 1932, Translation in NACA TT F-10

[Oti03] Otić, I., Grötzbach, G.,
Direct numerical simulation and statistical analysis of turbulent convection in lead-bismuth.
International Conference on Supercomputing in Nuclear Applications, SNA 2003, Paris, Sept. 22-24, 2003, Gif sur Yvette : CEA 2003, CD-ROM paper Nr. S10/2

[Oti05] Otić, I., Grötzbach, G., Wörner, M.,
Analysis and modelling of the temperature variance equation in turbulent natural convection for low Prandtl number fluids.
J. Fluid Mech. 525, 2005, pp. 237-261

[Oti05a] Otić, I., Grötzbach, G.,
DNS based analysis and modelling of the turbulent heat transfer by natural convection in liquid lead-bismuth.
2005 ASME Summer Heat Transfer Conference, San Francisco, California, July 17-22, 2005. Proc. On CD-ROM: HT2005, Eds. R. Skocypec, C. Amon, ASME 2005, ISBN No. 0-7918-3762-9, ASME order Nr. I729CD

[Oti07] Otić, I., Grötzbach, G.,
Turbulent heat flux and temperature variance dissipation rate in natural convection in lead-bismuth.
Nucl. Sc. Engng. 155, 2007, pp. 489-496

[Piq99] Piquet, J.,
Turbulent Flows - Models and Physics.
Springer, Berlin 1999

[Qua72] Quarmby, A., Quirk, R.,
Measurements of the radial and tangential eddy diffusivities of heat and mass in turbulent flow in a plain tube.
Int. J. Heat Mass Transfer 15, 1972, pp. 2309-2327

[Qua74] Quarmby, A., Quirk, R.,
Axisymmetric and non-axisymmetric turbulent diffusion in a plain circular tube at high Schmidt number.
Int. J. Heat Mass Transfer 17, 1974, pp. 143-148

[Ramm75] Ramm, H., Johannsen, K.,
A phenomenological turbulence model and its application to heat transport in infinite rod arrays with axial turbulent flow.
J. Heat Trans. 97, 1975, pp. 231-237

[Ramm75a] Ramm, H., Johannsen, K.,
Prediction of local and integral turbulent transport properties for liquid metal heat transfer in equilateral triangular rod arrays.
J. Heat Trans. 97, 1975, pp. 238-243

[Reh92] Rehme, K.,
The structure of turbulence in rod bundles and the implications on natural mixing between the subchannels.
Int. J. Heat Mass Transfer 35, 1992, pp 567-581

[ReyA75] Reynolds, A.J.,
The prediction of turbulent Prandtl and Schmidt numbers.
Int. J. Heat Mass Transfer 18, 1975, pp. 1055 1069

[Rodi87] Rodi, W.,
Examples of calculation methods for flow and mixing in stratified fluids.
J. Geophys. Res. 92, 1987, pp. 5305-5328

[Rodi93] Rodi, W.,
Turbulence models and their application in hydraulics - A state of the art review.
IAHR publication, Delft, Balkema Rotterdam, 3rd ed., 1993.

[Sab01] Sabisch, W., Wörner, M., Grötzbach, G., Cacuci, D. G.,
3d Volume-of-Fluid simulation of a wobbling bubble in a gas-liquid system of low Morton number.
Fourth International Conference on Multiphase Flow, ICMF-2001, New Orleans, Louisiana, USA, May 27 - June 1, 2001, Ed. E.E. Michaelides, CD-ROM, paper 244.

[Sam96] Samstag, M.,
Experimentelle Untersuchungen von Transportphänomenen in vertikalen turbulenten Luft-Wasser-Blasenströmungen.
Dissertation, Univ. Karlsruhe, FZKA 5662, Forschungszentrum Karlsruhe 1996

[Sch75] Schumann, U.,
Subgrid scale modeling for finite difference simulations of turbulent flows in plane channels and annuli.
J. Comp. Phys. 18, 1975, pp. 376-4o4

[Sch80] Schumann, U., Grötzbach, G., Kleiser, L.,
Direct numerical simulation of turbulence.
Prediction Methods for Turbulent Flows. Ed. W. Kollmann, Hemisphere Publ. Co., Washington 1980, pp. 123-258.

[Sch87] Schumann, U.,
The counter-gradient heat flux in turbulent stratified flows.
Nucl. Engng. Design 100, 1987, pp. 255-262

[Schb05] Schulenberg, T., Cheng, X., Stieglitz, R.,
Thermal-hydraulics of lead bismuth for accelerator driven systems.
Proc. of the 11th Internat. Topical Meeting on Nuclear Reactor Thermal-Hydraulics, NURETH-11, Avignon, F, October 2-6, 2005, CD-ROM paper 159

[Schl65] Schlichting, H.,
Grenzschichttheorie.
Verlag G. Braun, Karlsruhe 1965

[SchL76] Schemm, C.E., Lipps, F.B.,
Some results from a simplified three dimensional numerical model of atmospheric turbulence.
J. Atmos. Sci. 33, 1976, pp. 1021-1041

[Schw06] Schwertfirm, F., Manhart, M.,
DNS of passive scalar transport in turbulent channel flow at high Schmidt numbers.
Turbulence, Heat and Mass Transfer 5, Ed. K. Hanjalić, Y. Nagano, S. Jakirlić, Begell House Inc. 2006, pp. 289-292

[Schw07] Schwertfirm, F., Manhart, M.,
DNS of passive scalar transport in turbulent channel flow at high Schmidt numbers.
Int. J. Heat Fluid Flow 28, 2007, pp. 1204-1214,
DOI: 10.1016/j.ijheatfluidflow.2007.05.012, 2007

[Som76] Sommeria, G.,
Three dimensional simulation of turbulent processes in an undisturbed trade wind boundary layer.
J. Atmos. Sci. 33, 1976, pp. 216 241

[Star06] STAR-CD-Version 4.02.,
Methodology.
CD-adapco, 2006

[Sti07] Stieglitz, R., Daubner, M., Batta, A., Lefhalm, C.H.,
Turbulent heat mixing of a heavy liquid metal flow in the MEGAPIE target geometry. The heated jet experiment.
Nucl. Engng. Design 237, 2007, pp. 1765-85

[Ties98] Tieszen, S., Ooi, A., Durbin, P., Behnia, M.,
Modeling of natural convection heat transfer.
Center for Turbulence Research, Stanford, CA, USA, Proc. Summer Program 1998, pp. 287-302

[Ven03] Venayagamoorthy, S.K., Koseff, J.R., Ferziger, J.H., Shih, L.H.,
Testing of RANS turbulence models for stratified flows based on DNS data.
Annual Research Briefs, Center for Turbulence Research, Stanford, CA, USA, 2003, pp. 127-138

[Wil96] Willerding, G., Baumann, W.,
FLUTAN 2.0 - Input specifications.
FZKA 5712, Forschungszentrum Karlsruhe 1996

[Wör93] Wörner, M., Grötzbach, G.,
Turbulent heat flux balance for natural convection in air and sodium analysed by direct numerical simulations.
5th Int. Symposium on Refined Flow Modelling and Turbulence Measurements, Paris, France, Sept. 7-10, 1993, Paris : Presses de l' Ecole Nationale des Ponts et Chaussees, 1993, pp. 335-342

[Wör94] Wörner, M.,
Direkte Simulation turbulenter Rayleigh-Bénard Konvektion in flüssigem Natrium.
Dissertation, Univ. Karlsruhe, KfK 5228, Kernforschungszentrum Karlsruhe 1994

[Wör95] Wörner, M., Grötzbach, G.,
Analysis of thermal variance equation for natural convection of air and sodium.
Turbulence, Heat and Mass Transfer 1, Proc.of the Internat.Symp., Lisboa, P, August 9-12, 1994, Ed. K. Hanjalić, J.C.F. Pereira, Begell House Inc., N.Y., 1995, pp. 332-337

[Wör95a] Wörner, M., Grötzbach, G.,
Modelling the molecular terms in the turbulent heat flux equation for natural convection.
Proceedings Tenth Symposium on Turbulent Shear Flows, University Park, PA, USA, August 14-16, 1995, Pennsylvania State University, State College, Pennsylvania, USA, Vol. 2, pp. P2-73 - P2-78

[Wör97] Wörner, M., Schmidt, M., Grötzbach, G.,
DNS of turbulence in an internally heated convective fluid layer and implications for statistical modelling.
J. Hyd. Res. 35, 1997, pp. 773-797

[Wör97a] Wörner, M., Grötzbach, G.,
DNS database of turbulent natural convection in horizontal fluid layers. Forschungszentrum Karlsruhe,
http://www.iket.fzk.de/TURBIT
February 1997

[Wör98] Wörner, M., Grötzbach, G.,
Pressure transport in direct numerical simulations of turbulent natural convection in horizontal fluid layers.
Int. J. Heat Fluid Flow 19, 1998, pp. 150-158

[Wör99] Wörner, M., Ye, Q.-Y., Grötzbach, G.,
Consistent modelling of fluctuating temperature-gradient-velocity-gradient correlations for natural convection.
Proc.of the 4th Internat.Symp., Ajaccio, F, May 24-26, 1999 : Engineering Turbulence Modelling and Experiments 4, Eds. W. Rodi, D. Laurence, Elsevier Science B. V., Amsterdam, 1999, pp. 165-174.